NACA TN 4091

425

NATIONAL ADVISORY COMMITTEE
FOR AERONAUTICS

TECHNICAL NOTE 4091

EXPERIMENTAL INVESTIGATION OF TRANSPIRATION COOLING FOR

A TURBULENT BOUNDARY LAYER IN SUBSONIC FLOW

USING AIR AS A COOLANT

By William E. Brunk

Lewis Flight Propulsion Laboratory
Cleveland, Ohio

NACA

Washington
October 1957

4297

CI-1

NATIONAL ADVISORY COMMITTEE FOR AERONAUTICS

TECHNICAL NOTE 4091

EXPERIMENTAL INVESTIGATION OF TRANSPIRATION COOLING FOR A

TURBULENT BOUNDARY LAYER IN SUBSONIC

FLOW USING AIR AS A COOLANT

By William E. Brunk

SUMMARY

Experiments were performed to determine the effect of injecting coolant air through a porous sintered bronze plate into a constant-area tunnel through which hot air was flowing. The boundary layer was turbulent over the porous plate for all test runs. Tests were made with either a constant coolant injection rate or a constant wall temperature. The Mach number was approximately 0.6 at the upstream edge of the porous plate and increased in the downstream direction. The mainstream stagnation temperature was approximately 215° F, and the coolant temperature was either in the range -15° to 5° F or the range -70° to -55° F.

It was difficult to run at the desired injection flow conditions, because the permeability of the sintered bronze plate varied erratically with both time and position. Nevertheless, a definite correlation existed between the porous wall temperature and the injected coolant-flow rate; wall temperature decreased as coolant-flow rate increased. This correlation for a given station along the porous plate appeared independent of the type of test when based on local conditions. A comparison of the results with a theory for transpiration into a turbulent boundary layer with an isothermal wall showed only qualitative agreement. This was not unexpected, since some of the important assumptions of the theory could not be completely satisfied in the experimental setup.

INTRODUCTION

The problem of cooling a surface in contact with hot gases has become increasingly important. Several methods of cooling have been studied. In reference 1, an analytical comparison of convection cooling, film cooling, and transpiration cooling showed transpiration cooling to be the most efficient method of the three. In transpiration cooling, the coolant is passed through the heated surface and injected directly into

the boundary layer. This requires that the heated surface be constructed of a porous material.

A number of experimental studies on transpiration cooling are reported in the literature. Both references 2 and 3 are concerned with the injection of air into a laminar boundary layer with low subsonic mainstream velocities. In both of these papers, the temperature difference between the mainstream flow and the injected air was either small or negligible. However, in reference 4 transpiration-cooling information was obtained for mainstream temperatures of approximately 2000° and 4000° F and high subsonic velocities. In these experiments nitrogen and hydrogen were used as coolants, and the porous surfaces were made of copper, nickel, or stainless steel. The effect of transpiration cooling was found to depend upon the nature of the porous material of which the heated surface was constructed and also upon the gas used as a coolant.

The results of an investigation of the effect of injecting a coolant through a porous surface into a turbulent boundary layer are presented herein. Both the coolant and mainstream gases are air, and the mainstream velocities are subsonic.

SYMBOLS

c_p specific heat at constant pressure

k thermal conductivity

Pr Prandtl number, $c_p\mu/k$

Re_l Reynolds number based on length of porous plate

r $2.11/Re_l^{0.1}$

S surface area of porous plate covering duct

T temperature

T_{aw} adiabatic wall temperature for solid flat plate

u velocity in x-direction

v velocity in y-direction

x distance parallel to porous wall in direction of tunnel flow

y distance perpendicular to porous wall and into tunnel

μ   absolute viscosity

ρ   density

φ $\dfrac{(\rho v)_c Re_l^{0.2} Pr_\infty^{2/3}}{0.037 (\rho u)_\infty}$

Subscripts:

av   based on average conditions

c   coolant

d   duct number

w   stream side of porous plate

l   duct 1

∞   free stream

APPARATUS AND PROCEDURES

The experimental work presented in this report was performed in a 4-by 10-inch continuous-flow wind tunnel at the NACA Lewis laboratory. The tunnel was modified to permit injection of a coolant by replacing one of the vertical 10-inch tunnel walls with a special wall as shown in figure 1. This wall, here referred to as the test wall, was composed of five sections. The upstream section, approximately 24 inches long, was of solid polished stainless steel. The next section, a Lektromesh screen 8 inches across, was followed by a solid piece of stainless steel 1/4 inch wide. A 60-inch-long porous bronze plate and a solid polished stainless-steel section completed the test wall. The three other walls of the tunnel were of solid stainless steel plated with approximately 0.003 inch of pure silver, which was highly polished. The silver plate minimized heat transfer from these walls by radiation.

An auxiliary ducting system was built for injecting the coolant air into the tunnel through the porous plate. A top view of this system is shown in figure 2. Figure 2 also shows the boundary-layer-bleed exhaust system. Each of these special components is fully described in the following sections.

Porous Plate

The porous section of the test wall consisted of a 1/2-inch-thick sintered bronze plate that was manufactured in one continuous piece. The

face of the plate towards the interior of the tunnel (herein referred to as the stream side of the plate) was flat, with an average surface roughness of 0.0005 inch. The emissivity of a sample of the plate material (ref. 5) was 0.54±5 percent up to a temperature of 350° F.

The original specifications required that the permeability of the porous plate be such that, when a pressure drop of 8 pounds per square inch was maintained across the plate, a uniform mass flow of 0.55 pound per square foot per second be obtained within ±8 percent. Since it was not possible to measure permeability over an arbitrarily small area, all permeabilities measured were averages over a circular area 7/8 inch in diameter. When the plate was received from the manufacturer, the permeability was found to be within the specifications. However, after air was passed through the plate for a few hours, the plate became plugged in spots because of dirt in the air. A second examination revealed that the permeability variations were far greater than originally specified.

After the plate was instrumented but before it was mounted in the test wall, it was cleaned in a vapor bath of trichloroethylene. A final examination showed the permeability variation to be again within specifications. However, permeability checks made at intervals during the period of the tests showed that the permeability changed from run to run and that the variation was not uniform. An unsuccessful attempt was made to clean the plate while it was mounted in the tunnel. Figures 3(a) and (b) show the relative permeability along the horizontal centerline of the tunnel and along the vertical centerlines of some of the ducts, respectively. The circles represent the relative permeability just before the first run, and the squares just after the last run. The relative permeability at a test location is given as the ratio of the local permeability to the average permeability over the given duct. The permeability was not more uniform before the first run because the plate had become partially plugged during the preliminary test runs.

Coolant System

In order to inject coolant air through the porous plate, a system of coolant-air ducts was constructed. A top view of this system is shown in figure 2, and a vertical cross section of an individual duct is shown in figure 4. The width of the individual ducts was designed so that the coolant air could be injected to give a constant wall temperature. The ducts were connected to a refrigerated-air line by means of the common manifold shown in figure 2. The amount of air flowing into each duct was controlled by an electrically operated butterfly valve in the line between the manifold and the duct.

To ensure that the flow of air entering the porous plate would be uniform for each duct, two screens were placed in each duct to spread the

flow (fig. 4). One screen was placed at the end of the pipe leading into
the duct, and the other screen was placed halfway between the pipe and
the porous plate. A survey showed that the flow entering the porous plate
was uniform with this arrangement.

There was a knife-edge contact between the edges of the ducts and
the porous plate. As the coolant side of the porous plate (the side op-
posite the stream side) was not smooth, the seal between the ducts and
the plate was not perfect. To prevent loss of coolant flow, the cracks
between the ducts were filled with a sealing material. Nevertheless, a
small flow of air between ducts always existed because of pressure
differences.

Boundary-Layer Bleed

In order to control the size of the boundary layer on the test wall
at the upstream edge of the porous plate, a boundary-layer-bleed system
was constructed immediately upstream of the porous plate. The bleed sys-
tem consisted of a duct leading from the test wall of the tunnel to the
tunnel exhausters, through which suction could be applied. The tunnel
end of the duct was covered by a Lektromesh screen.

Tests made with the tunnel running at average conditions showed the
boundary-layer thickness at the upstream edge of the porous plate to vary
between 0.40 inch with no suction and 0.01 inch with maximum suction.
For maximum suction it was assumed that the boundary layer effectively
started at the upstream edge of the porous plate. These two conditions
were used for running the final tests.

Instrumentation

The tunnel, test wall, and coolant system were instrumented to deter-
mine (1) the mass flow in the tunnel, (2) the mass flow through each of
the coolant ducts, (3) the temperature on each side of the porous plate,
(4) the temperature of the coolant just before entering the porous plate,
and (5) the temperature of the wall opposite the porous plate.

The mass flow in the tunnel was calculated from measurements of
total and static pressure and stagnation temperature at the upstream end
of the porous plate. Orifices on the wall opposite the porous plate gave
the static-pressure distribution along the tunnel. The mass flow through
the coolant ducts was determined by previously calibrating mass flow meas-
ured by a rotameter against the Reynolds number based on static pressure,
stagnation temperature, and a single Pitot pressure.

The temperature of the coolant just before it entered the porous
plate was given by a single temperature probe in each duct 1 inch from

the coolant side of the porous plate. The temperature of the wall oppo-
site the porous plate was measured by thermocouples mounted in the wall.

The temperature on each side of the porous plate was measured by
thermocouples mounted in the plate. The method of mounting these thermo-
couples is shown in figure 5. At the position where a thermocouple was
to be mounted, a small groove 1/16 inch deep, 1/16 inch wide, and 1/2 inch
long was carefully cut into the porous plate. A thermocouple was placed
in each groove with the junction at one end and with the wire running
along the groove. The wire was then led away from the plate to reduce
errors due to conduction on the plate surface. The leads on the thermo-
couples mounted on the stream side of the porous plate were passed through
a small hole drilled in the end of the groove and led directly away from
the coolant side of the plate. In each of the ducts two thermocouples
were mounted on the vertical centerline of the duct 1 inch below the
horizontal centerline, the central thermocouple being mounted on the
stream side and the other on the coolant side of the porous plate. In
each of ducts 1, 3, 5, 7, and 8, two additional thermocouples were mounted
on the vertical centerline on the stream side of the porous plate, one
$2\frac{1}{2}$ inches above and the other $2\frac{1}{2}$ inches below the horizontal centerline.
These thermocouples were installed to determine flow uniformity. The
location of thermocouples in ducts 1, 3, 5, 7, and 8 is shown in figure
4. All thermocouples were connected to a Brown recorder. Temperatures
were read in millivolts and then converted to degrees.

Operating Conditions

The total pressure in the tunnel during the runs ranged from 38 to
41 inches of mercury absolute, while the total pressure in the coolant
air line was 50 inches of mercury absolute. Because of the varying amount
of coolant air injected into the tunnel, the Mach number at the upstream
end of the porous plate ranged from 0.53 to 0.65. The Mach number in-
creased in the downstream direction because of a static-pressure decrease
along the tunnel, as shown in figure 6 for a typical run. The tunnel
inlet temperature was kept within the range of 205° to 230° F, although
for a few runs it was lowered to the range of 110° to 150° F. The cool-
ant air was available in either one of two ranges, a high range of -15°
to 5° F or a low range of -70° to -55° F. Although it was possible to
choose the desired range of coolant temperature, it was not possible to
fix the temperature more closely.

Test Procedure

Two basically different types of runs were made: (1) The temperature
along the stream side of the porous plate was kept constant, and (2) the
amount of coolant mass flow injected per unit area along the porous plate
was kept constant.

For the constant-wall-temperature runs, the amount of coolant air injected into the main stream through each duct was adjusted until the central thermocouples indicated the same temperature along the entire plate. To accomplish this, the main tunnel flow was first set at the desired conditions and the boundary-layer bleed was adjusted to give the desired boundary-layer thickness at the upstream edge of the porous plate. Duct 1 was then fully opened and all the other ducts were slightly opened. Then duct 2 was opened until the apparent temperature (the temperature indicated by the central thermocouple) of the stream side of the porous plate reached approximately the desired value. The flow through each of the succeeding ducts was then adjusted until each central thermocouple indicated approximately the same temperature. A change in the amount of flow through any duct produced a temperature change in the porous plate covering the adjacent ducts. This change was the most pronounced in the downstream direction. Therefore, it was necessary to readjust the injected coolant flow several times before all the central thermocouples registered the same temperature. The tunnel was then run for several minutes to reach equilibrium. Any small changes in the thermocouple readings were corrected by adjusting the amount of injected coolant flow. After all the conditions remained constant for more than 15 minutes, data were taken.

For the constant-mass-flow runs, the rate of coolant mass flow through each duct was adjusted to give a constant mass flow per unit area through all the ducts. To accomplish this the tunnel was set at the desired conditions and the boundary-layer bleed was adjusted as in the constant-wall-temperature runs. The butterfly valves for each duct were then opened until the correct rate, based on calculations, of coolant mass flow through each duct was reached. The tunnel was allowed to run until an equilibrium state was reached, and then data were taken.

## RESULTS AND DISCUSSION

Constant Wall Temperature

With the apparent (central thermocouple) temperature of the stream side of the porous plate held approximately constant, runs were made (a) with no boundary-layer bleed and (b) with maximum boundary-layer bleed. The apparent temperature distribution along both the stream and coolant sides of the porous plate is shown in figure 7(a) for a typical run with no boundary-layer bleed. A similar curve is shown in figure 7(b) for a typical run with maximum boundary-layer bleed. The lines connecting the data points in figure 7 are dashed, since they do not necessarily represent the actual temperature distribution along the plate. Figures 8(a) and (b) give the relative coolant mass flow per unit area through each duct for the same respective runs.

It was not possible to adjust the coolant-flow rate to give a con-
stant apparent temperature along the entire porous plate. For the runs
with no boundary-layer bleed, the apparent temperature of the porous
plate over duct 2 was always lower than that of the plate over duct 1.
When there is no flow through duct 2, the mainstream pressure gradient
causes the coolant flow through duct 1 to travel diagonally through the
porous plate and partially cover duct 2, as shown in sketch (a). When

Porous plate

Duct   Duct   Duct
1   2   3
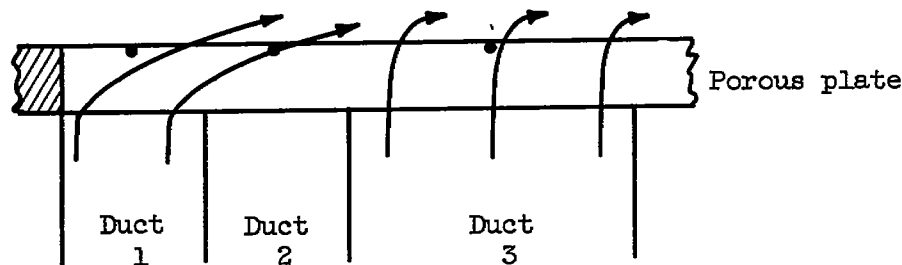
(a)

coolant flow is passed through duct 2, the coolant from duct 1 is dis-
placed as in sketch (b), so that the coolant flow through duct 1 lowers
the apparent temperature of the porous plate over duct 1. The apparent

Porous plate

Duct   Duct   Duct
1   2   3
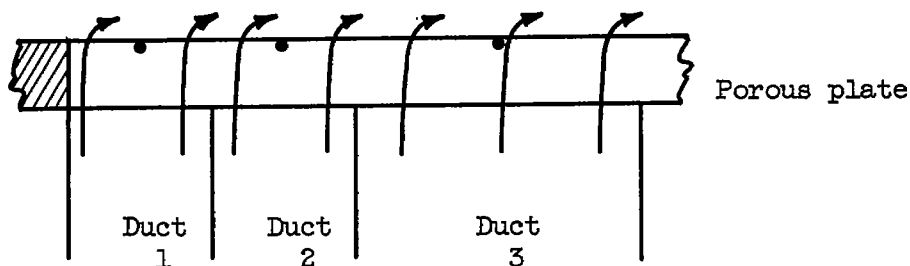
(b)

temperature of the porous plate over duct 2 is lower than that over duct
1, because it is cooled by part of the duct 1 coolant as well as the duct
2 coolant, while only the remaining portion of duct 1 coolant acts on the
porous surface over duct 1. The apparent temperature of the porous plate
downstream of duct 2 could be set at any desired value without difficulty.

For the runs with maximum boundary-layer bleed where the boundary
layer effectively started at the upstream edge of the porous plate, the
rate of heat transfer to the plate covering the first duct was so great
that a very large flow of coolant air would have been necessary to keep

4297

the stream side of the porous plate at the desired temperature. There
were, however, two physical limitations on the coolant flow through the
upstream ducts. First, an upper limit to the amount of coolant flow
through a duct was set by the maximum pressure drop across the porous
plate; and second, the coolant air in the upstream ducts was heated slight-
ly by heat transfer from the hot air passing through the boundary-layer-
bleed system. These limitations were noticeable in ducts 1 and 2. For
the ducts downstream of duct 2, the desired porous-plate temperature could
be obtained easily.

The data presented in figure 8 are in disagreement with theory, which
predicts a decrease of coolant flow in the downstream direction. This
discrepancy can be explained by the variation in permeability of the po-
rous plate covering a single duct. The temperature of the porous plate
at any thermocouple depended on both the amount of coolant flow through
the duct and the permeability of the porous plate in the immediate neigh-
borhood of the thermocouple. If the permeability at the thermocouple was
lower than the average permeability for the porous plate covering the
duct, a greater amount of coolant flow was needed through the duct to
bring the temperature at the thermocouple to the desired value. This is
easily seen in duct 8, where the permeability at the center thermocouple
(see fig. 3(b)) is very low. Figure 8 shows that the amount of mass flow
through duct 8 was much greater than expected.

Constant Mass Flow

A few runs were made in which the rate of coolant mass flow per unit
area through the porous plate was kept approximately constant along the
entire plate. The rate of coolant mass flow per unit area through one
duct relative to the average mass-flow rate per unit area through all the
ducts is shown in figure 9 for a typical run. It is evident from this
figure that the actual mass-flow rate along the plate was not constant
for the run, because the pressures and temperatures could not be set ac-
curately in the coolant system. If, however, the theoretically desired
average mass flow per unit area through each duct could have been ob-
tained, the actual mass flow through each unit area of the porous plate
would have varied greatly because of the large variation in permeability.
The temperature distribution along the porous wall as obtained from the
central thermocouples is shown in figure 10 for the same run. The large
temperature increase at duct 8 is due to the extremely low permeability
at the location of the thermocouple. The lower temperature shown in the
figure gives the temperature at the upper thermocouple, where the rela-
tive permeability is near the average for the plate covering duct 8.

Variation of Wall Temperature with Coolant-Flow Rate

The effect of the rate of coolant flow on the wall temperature of
the porous plate is shown in figure 11. The data are presented as

temperature-difference ratio against mass-flow ratio. The temperature-
difference ratio is the ratio of the difference between the porous plate
temperature (stream side) and the coolant temperature 1 inch behind the
porous plate to the difference between the adiabatic wall temperature for
a solid flat plate based on a recovery factor for a turbulent boundary
layer and the coolant temperature. The mass-flow ratio is the ratio of
the injected coolant airflow per unit area to the local mainstream mass
flow per unit area. Local free-stream conditions were used, and the data
points from all the different types of runs are presented in the same
figure.

No attempt was made to plot the data points for ducts 1 and 2, as
there was no correlation between wall temperature and coolant mass flow
for these ducts. In duct 3 a slight correlation existed, as is shown in
figure 11(a), but the data points have a large, apparently random spread.
The results from the constant-mass-flow runs in figure 11(a) appear to
differ considerably from the rest of the points, but there is no known
reason for this difference. There is no systematic difference between
the data points for runs with no boundary-layer bleed and runs with maxi-
mum boundary-layer bleed. Since in the runs with no boundary-layer bleed
the boundary layer is turbulent at the position of duct 3, it can be as-
sumed either that the boundary layer is turbulent at this point with maxi-
mum boundary-layer bleed or that, for this type of correlation, no notice-
able difference between laminar and turbulent boundary layers is detect-
able with this experimental setup.

The curves for ducts 4 to 7 (figs. 11(b) to (e)) show a definite
correlation despite the fact that there is a rather large spread in the
data points. Except for a few widely scattered points, most of the data
points follow the same general curve independently of the type of run
from which they were obtained. This indicates that the wall temperature
apparently depends on conditions at the individual duct and is insensitive
to upstream conditions for mass-flow ratios greater than 0.002. There
is, however, one systematic difference ·in the data for all the ducts:
Data from runs with the low coolant temperature are generally shifted to
the right of the data from runs with the high coolant temperature.

The data points for the constant-mass-flow runs for duct 4 lie off
the general correlation curve. The reason for this will be explained
later.

The data points for duct 8 (fig. 11(f)) are considerably scattered,
and the constant-mass-flow data lie off the general correlation curve.
The wall temperature used for this plot is that indicated by the central
thermocouple, which, as has already been mentioned, indicates a tempera-
ture higher than the rest of the porous plate covering this duct. Fig-
ure 12 shows the data from duct 8 using the wall temperature as indicated
by the upper thermocouple, where the permeability is nearly equal to the
average for the porous plate covering the duct. The data points, which

4297

CI-2 back

had a considerable spread in figure 11(f), fall on a definite correlation curve in figure 12. The reason for this is the change in permeability at the thermocouples during the runs, as shown in figure 3(b). At the central thermocouple, 6 inches from the top, the relative permeability decreased appreciably during the runs; while at the upper thermocouple, 2.5 inches from the top, the relative permeability decreased only slightly. Thus, the constant-mass-flow data points, which were the last data taken, are spread out considerably from the data points taken near the beginning of the test runs. As the permeability at a point decreases, the wall temperature at the point rises, and therefore the temperature ratio becomes larger and the data points are shifted upwards. This is the reason for the general shift of the data points between figures 11(f) and 12 as well as for the data shift of duct 4.

The data points for ducts 4 to 8 are superimposed in figure 13. The constant-mass-flow points of duct 4 are omitted, along with a few points from the other ducts that fell completely off the correlation curves. The points shown for duct 8 are those from figure 12. Although the curves for the different ducts are shifted slightly with respect to each other, there is apparently no systematic shift among the data for the various ducts.

The experimental data for the runs with maximum boundary-layer bleed are compared in figure 14 with the theoretical result,

$$\frac{T_w - T_c}{T_{aw} - T_c} = \frac{1}{1 + \frac{Re_l^{0.1}}{2.11} (e^{r\varphi} - 1)}$$

where

$$r\varphi = \frac{2.11}{0.037} Re_l^{0.1} Pr_\infty^{2/3} \frac{(\rho v)_{c,av}}{(\rho u)_{\infty,av}}$$

The theory is for turbulent flow without radiation and is the one given in reference 1, in which the theory of reference 6 was used for the calculation of heat-transfer coefficients. The theory for zero radiation was used, since calculations showed that the ratio of the radiation heat-transfer coefficient to the convection heat-transfer coefficient was less than 10^{-3}. The coordinates of each experimental point in the figure are the temperature-difference ratio based on apparent porous-wall temperature, average coolant temperature, and adiabatic wall temperature for a flat plate with a turbulent boundary layer, and the mass-flow ratio $(\rho v)_{c,av}/(\rho u)_{\infty,av}$, where

$$(\rho v)_{c,av} = \frac{\sum_d (\rho v)_{c,d} S_d}{\sum_d S_d}$$

The summation is over all the ducts upstream of and including the duct in question, and $(\rho u)_{\infty,av}$ is based on average conditions along the tunnel from the upstream edge of the porous plate to the downstream end of the duct in question. Only the data for those runs where the tunnel conditions were approximately the same are plotted; therefore, the curves corresponding to given ducts are also constant Reynolds number curves based on plate length.

The experimental curves for constant Reynolds number and low coolant temperature in figure 14(b) are shifted slightly to the right of the corresponding curves for high coolant temperature in figure 14(a). This is the same coolant-temperature effect that was noticed in figures 11 to 13.

Although the curves for constant length Reynolds numbers agree qualitatively with the theoretical curves in figures 14(a) and (b), there is no quantitative agreement. The theory is based on the assumptions of constant mainstream velocity and a varying mass-flow rate to give constant temperature along the porous wall and hence no conduction along the wall. Neither of these assumptions was met in the experiments. Since the experiments were performed in a constant-area channel, a favorable pressure gradient existed with a consequent increase in velocity in the downstream direction. Likewise, for the reasons previously discussed, it was impossible to obtain the correct variation of coolant mass flow through the porous wall for a constant wall temperature; and it was not possible to compute corrections for the experimental data to approximate a constant wall temperature. If more coolant flow were injected through the first duct, then the average mass-flow ratio would increase. If the wall temperature did not change, this increased mass flow would shift the curves of constant Reynolds number to the right. However, additional coolant through the first duct would lower the temperature of that duct and the ducts farther downstream by increasing the thickness of the layer of cooler air along the plate. Thus, less coolant air would be needed through the downstream ducts, which would again reduce the average mass-flow ratio. Since these effects are interrelated, no general trends can be surmised.

CONCLUSIONS

The effect on the wall temperature of injecting cool air through a porous wall into a hot airstream for a turbulent boundary layer in subsonic flow has been studied experimentally. The following conclusions were reached:

1. The effectiveness of a sintered bronze plate as material for a porous wall depends on the lack of dirt and other foreign particles in the injected fluid. The porous plate used in these tests became plugged with dirt in a nonuniform manner when supposedly clean air was used as a coolant. The permeability of the plate, which was uniform at the beginning of the tests, varied from near the original value to almost zero at various points over the plate by the end of the tests.

2. By injecting the coolant through a series of ducts, it was possible to regulate the temperature along the porous wall. However, experimental limitations prevented obtaining the desired temperature at the upstream ducts, especially when the boundary layer started at the upstream edge of the porous plate.

3. The injection of the coolant had a large effect on the temperature of the hot side of the porous plate. The results indicate a definite correlation between wall temperature and local coolant-flow rate. For most of the ducts, the correlation is the same for runs with both constant wall temperature and constant coolant mass flow.

4. The experimental results agreed qualitatively with a previously suggested theory.

Lewis Flight Propulsion Laboratory
        National Advisory Committee for Aeronautics
                Cleveland, Ohio, July 15, 1957

REFERENCES

1. Eckert, E. R. G., and Livingood, John N. B.: Comparison of Effectiveness of Convection-, Transpiration-, and Film-Cooling Methods with Air as Coolant. NACA Rep. 1182, 1954. (Supersedes NACA TN 3010.)

2. Mickley, H. S., Ross, R. C., Squyers, A. L., and Stewart, W. E.: Heat, Mass, and Momentum Transfer for Flow over a Flat Plate with Blowing or Suction. NACA TN 3208, 1954.

3. Libby, Paul A., Kaufman, Lawrence, and Harrington, R. Paul: An Experimental Investigation of the Isothermal Laminar Boundary Layer on a Porous Flat Plate. Jour. Aero. Sci., vol. 19, no. 2, Feb. 1952, pp. 127-134.

4. Duwez, Pol, and Wheeler, H. L., Jr.: Experimental Study of Cooling by Injection of a Fluid Through a Porous Material. Jour. Aero. Sci., vol. 15, no. 9, Sept. 1948, pp. 509-521.

5. Eckert, E. R. G., Hartnett, J. P., and Irvine, T. F., Jr.: Measurement of Total Emissivity of Porous Materials in Use for Transpiration Cooling. Jet Prop., vol. 26, no. 4, Apr. 1956, pp. 280-282.

6. Friedman, Joseph: A Theoretical and Experimental Investigation of Rocket-Motor Sweat Cooling. Jour. Am. Rocket Soc., no. 79, Dec. 1949, pp. 147-154.
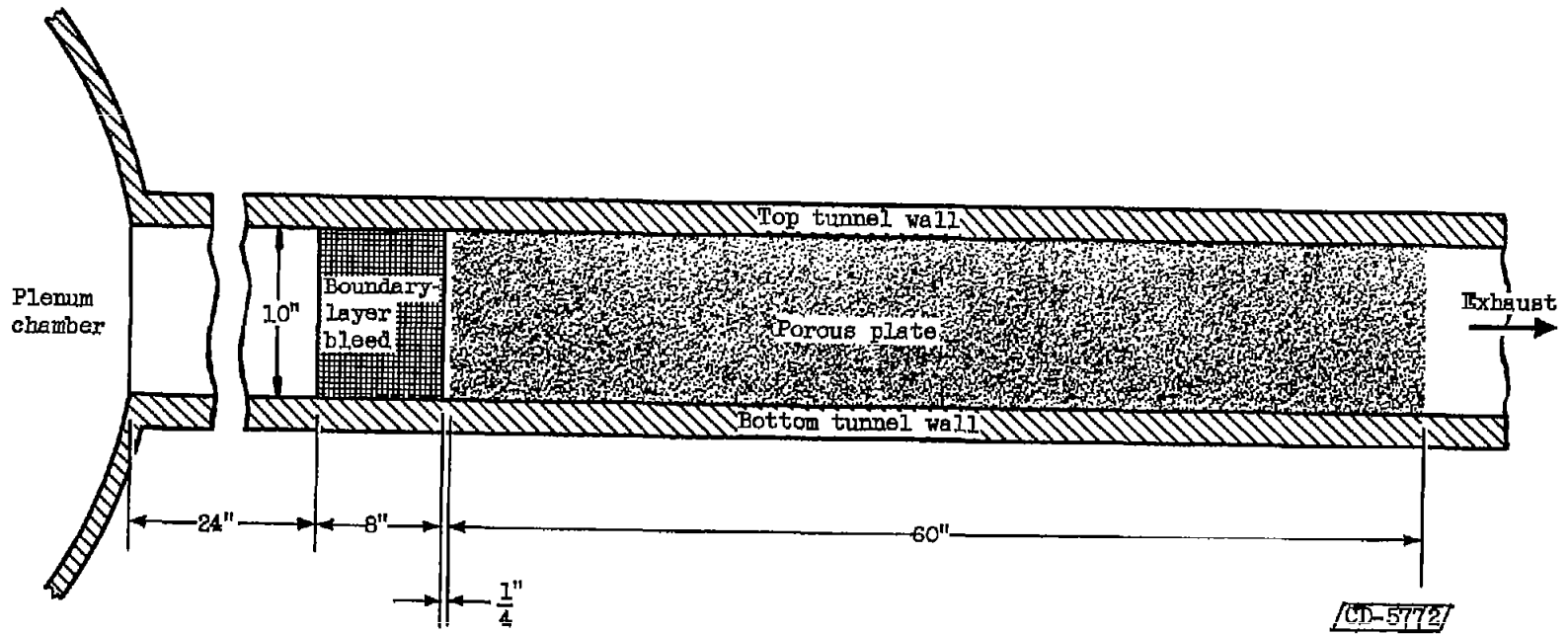
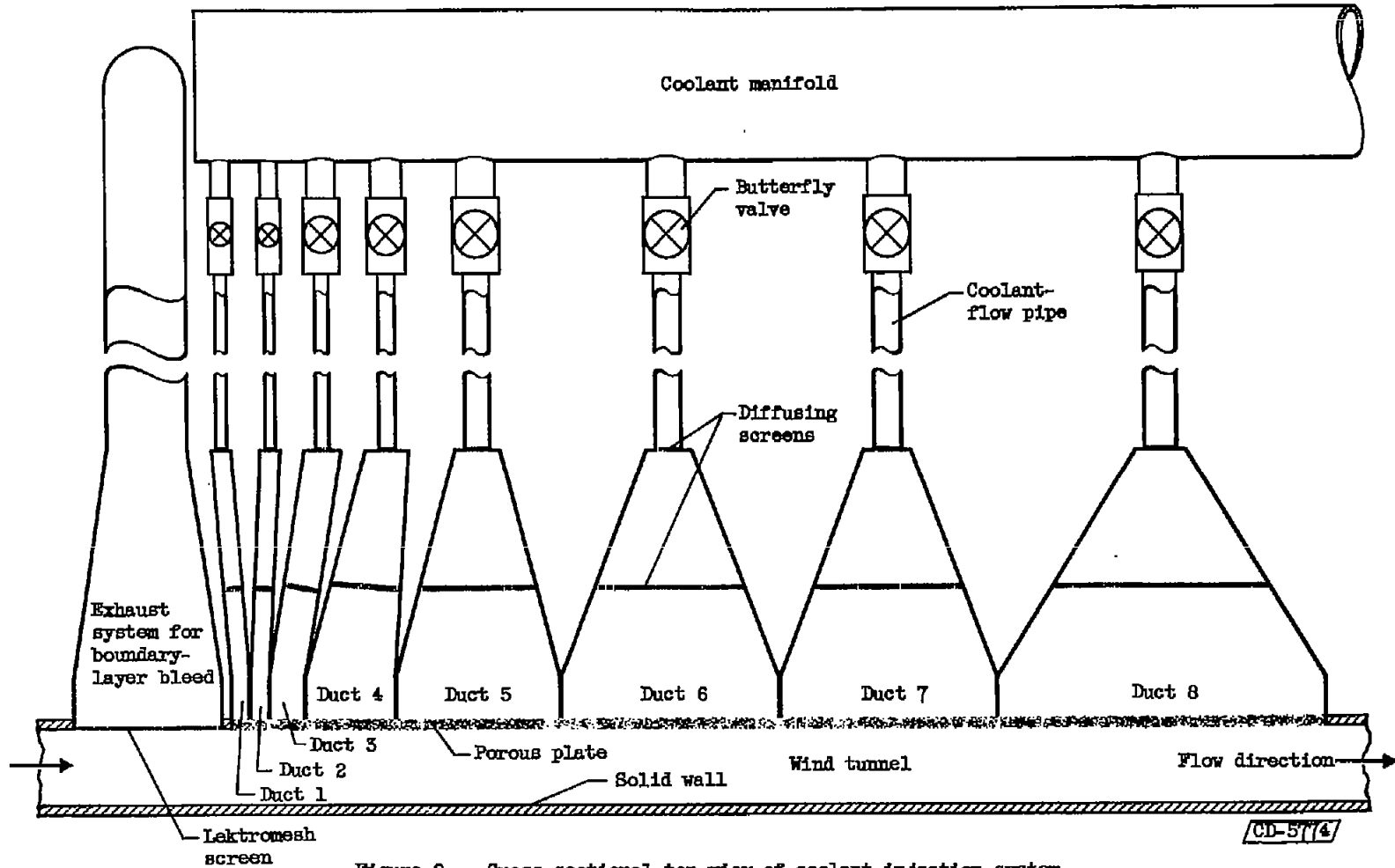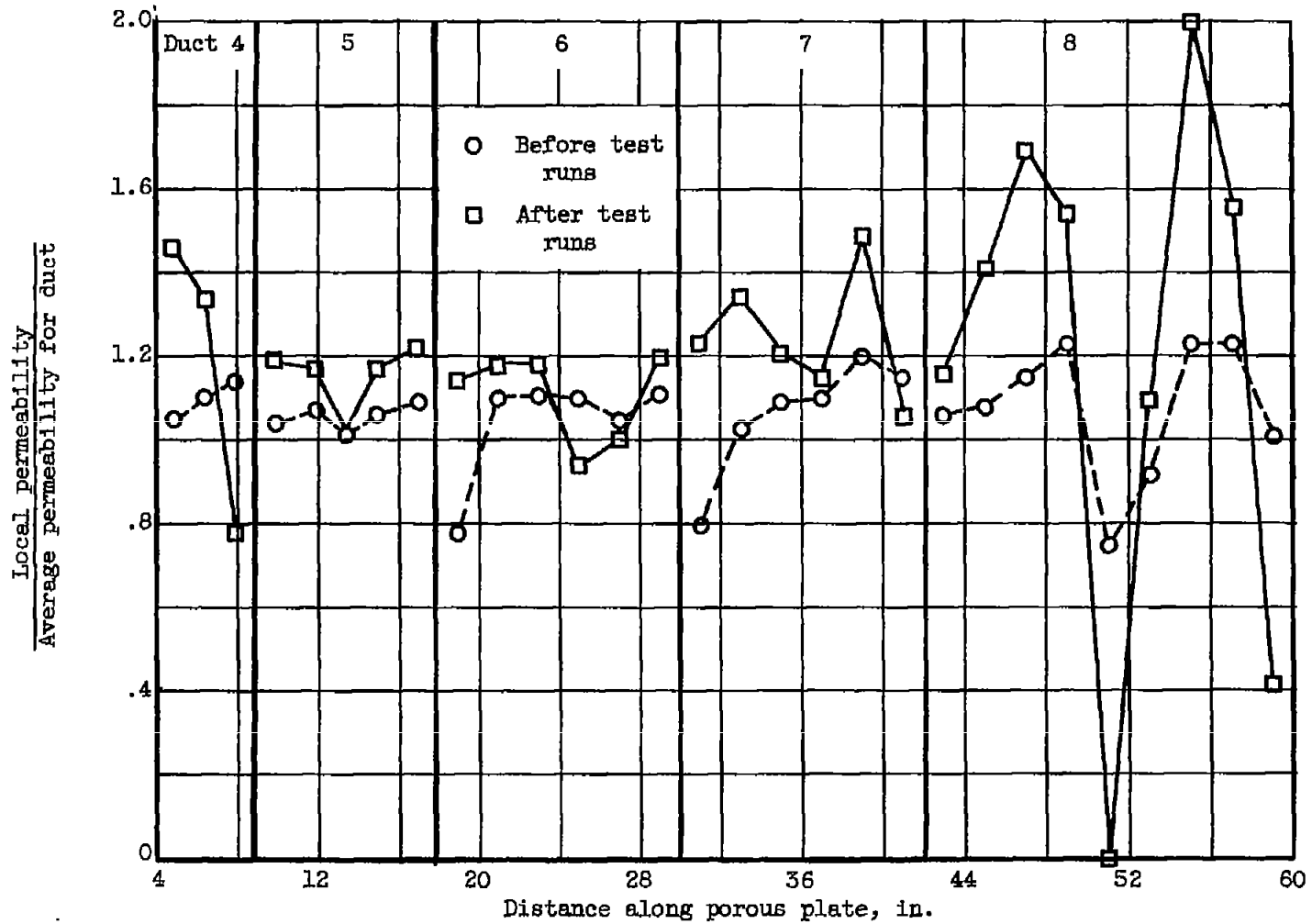Figure 1. - Cross section of tunnel showing position of porous plate in test wall.

Figure 2. - Cross-sectional top view of coolant injection system.

(a) Horizontal centerline of tunnel.

Figure 3. - Permeability variations of porous plate along centerlines of ducts 4 to 8 before and after test runs.

(b) Vertical centerlines of ducts.
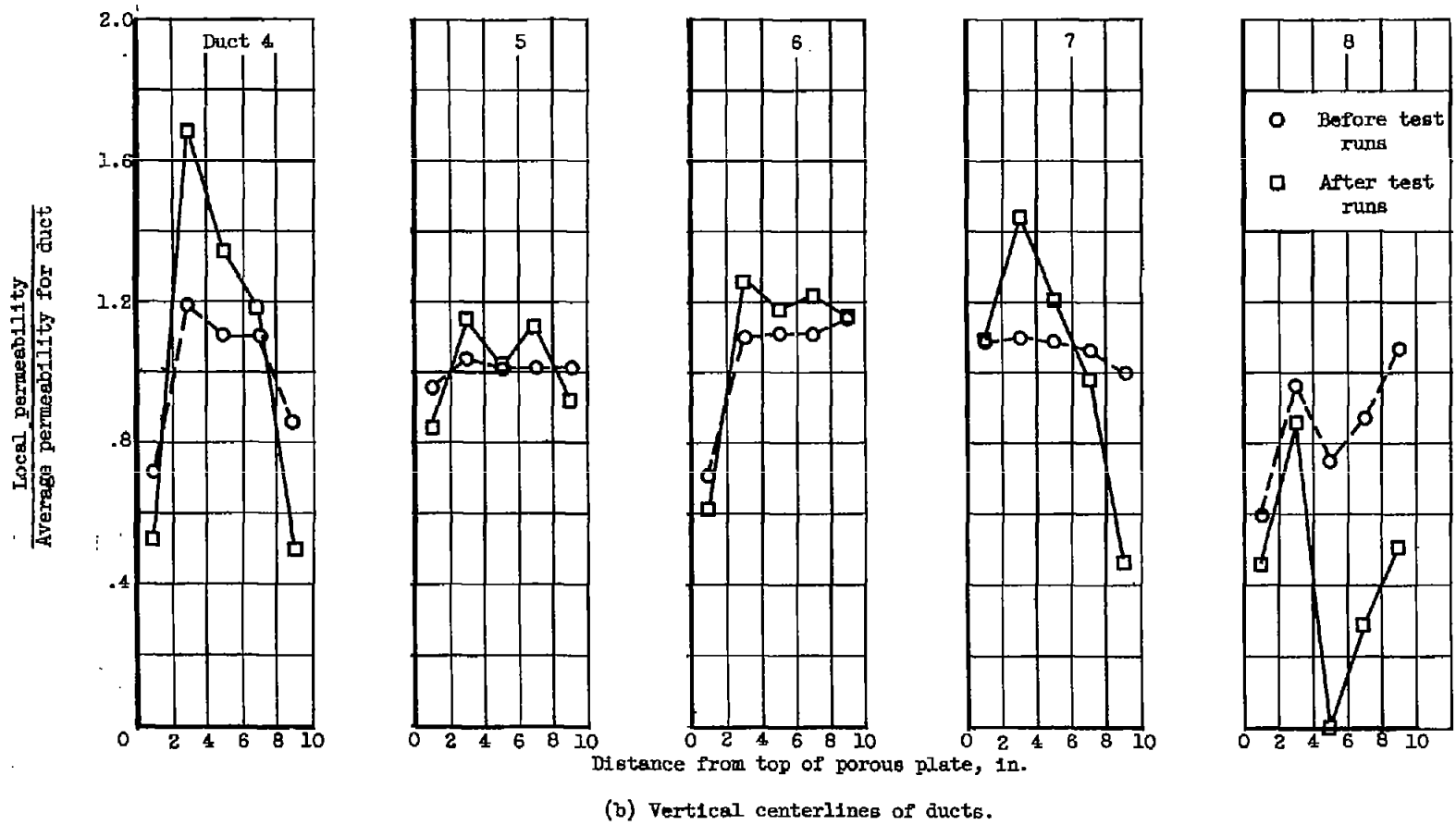
Figure 3. - Concluded. Permeability variations of porous plate along centerlines of ducts 4 to 8 before and after test runs.
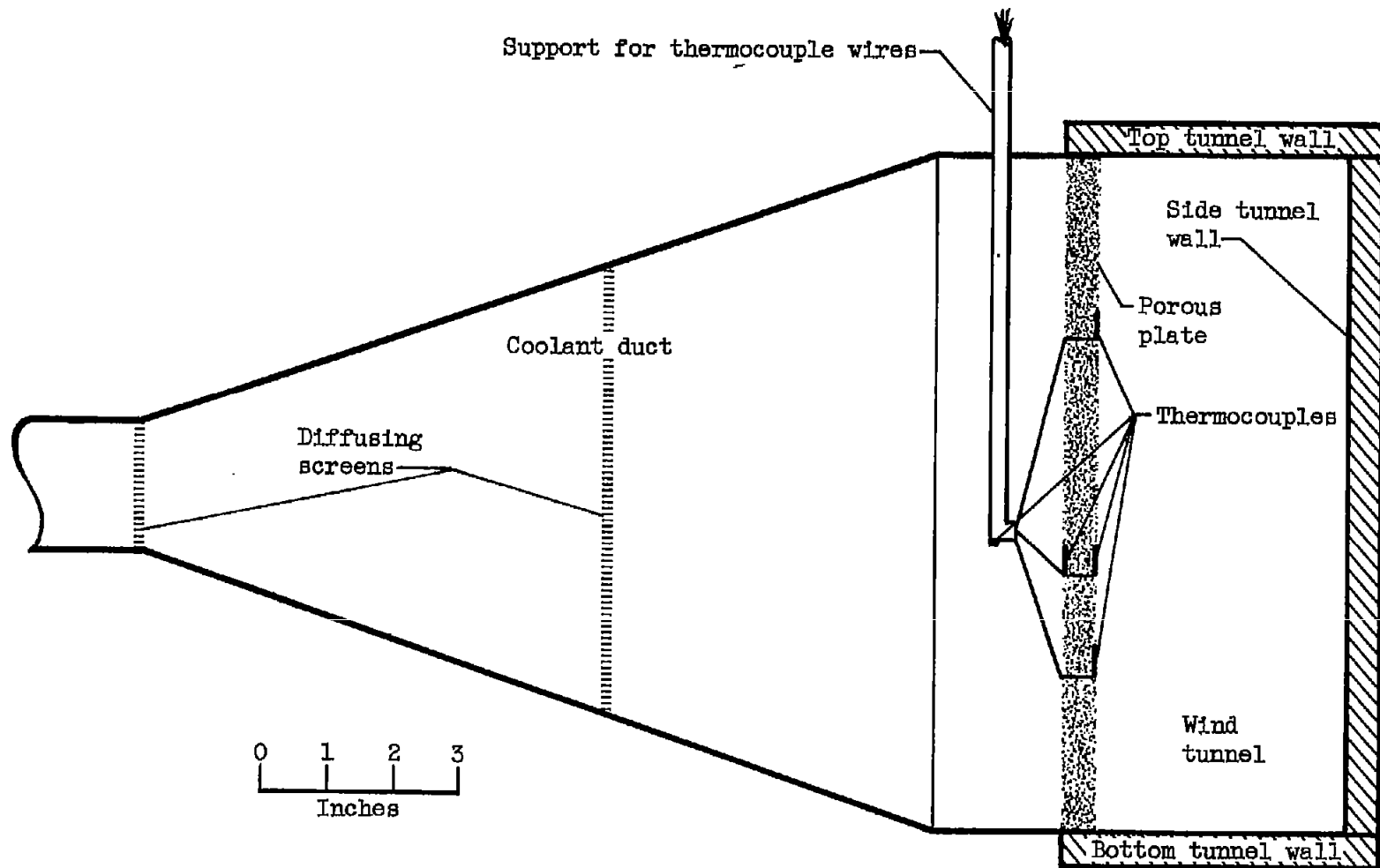
Figure 4. - Vertical cross section of typical coolant duct showing location of thermocouples as in ducts 1, 3, 5, 7, and 8.
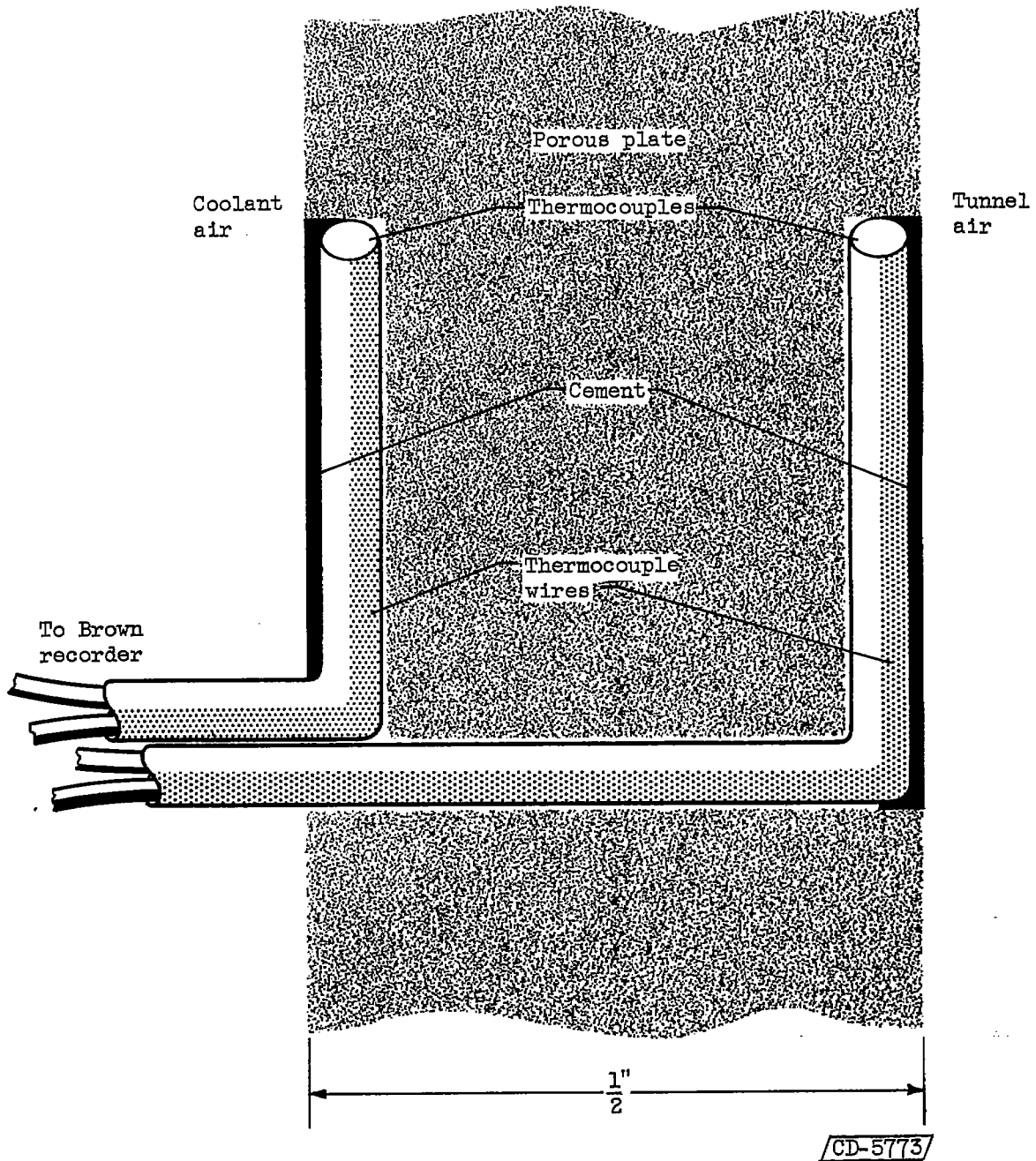
Figure 5. - Vertical cross section of porous plate showing method
of mounting thermocouples.
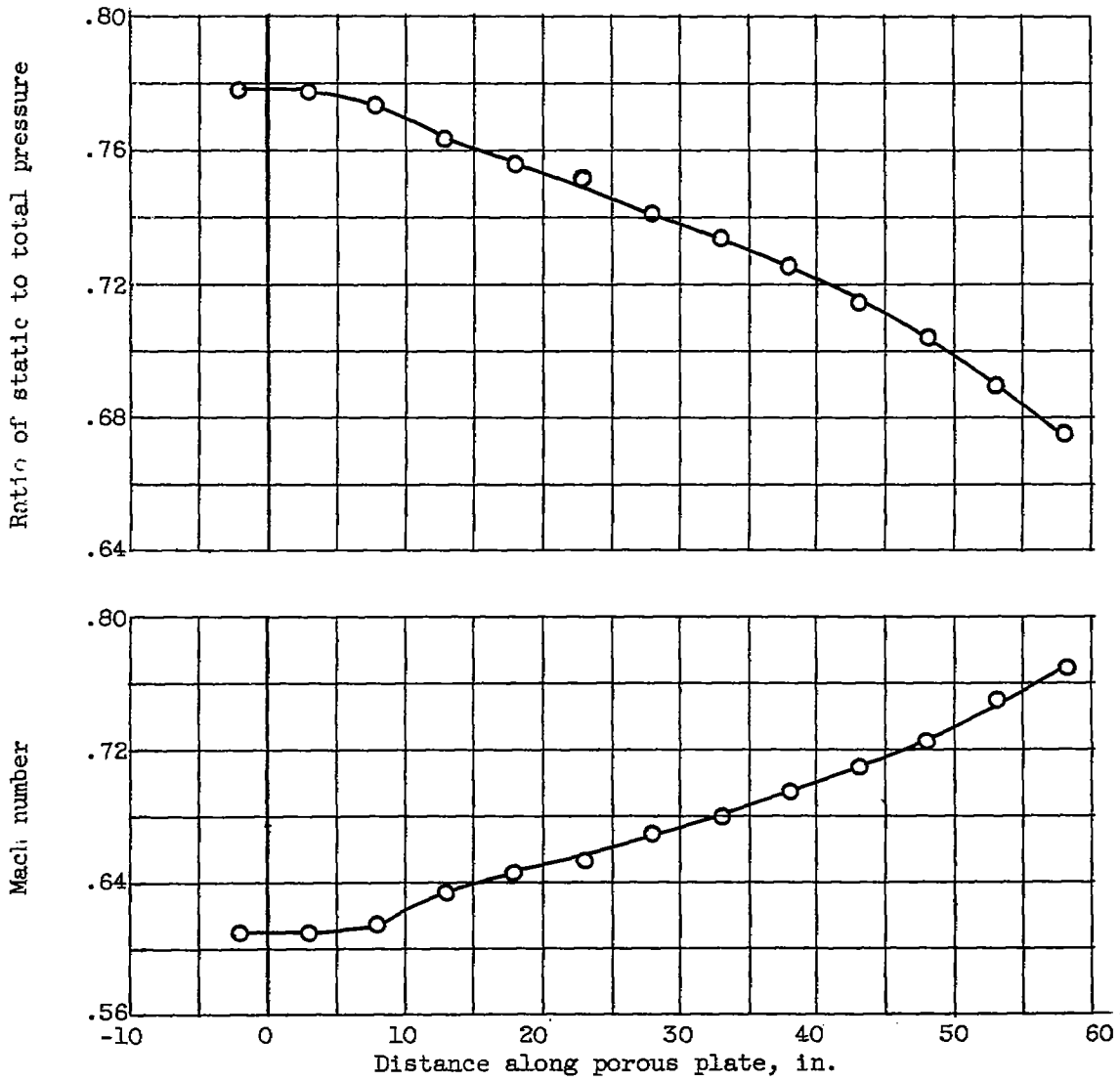
Figure 6. - Typical static-pressure and Mach number distributions
along tunnel with maximum boundary-layer bleed.
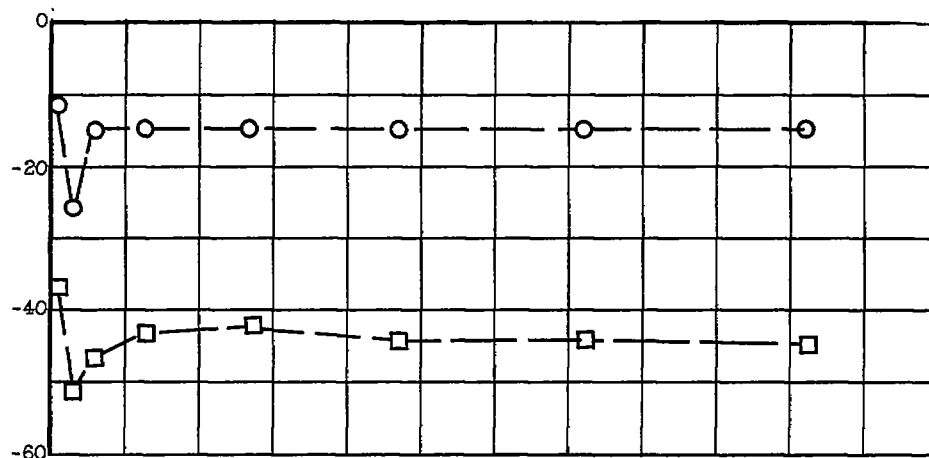
(a) No boundary-layer bleed. Stagnation temperature, 228° F.

O   Stream side
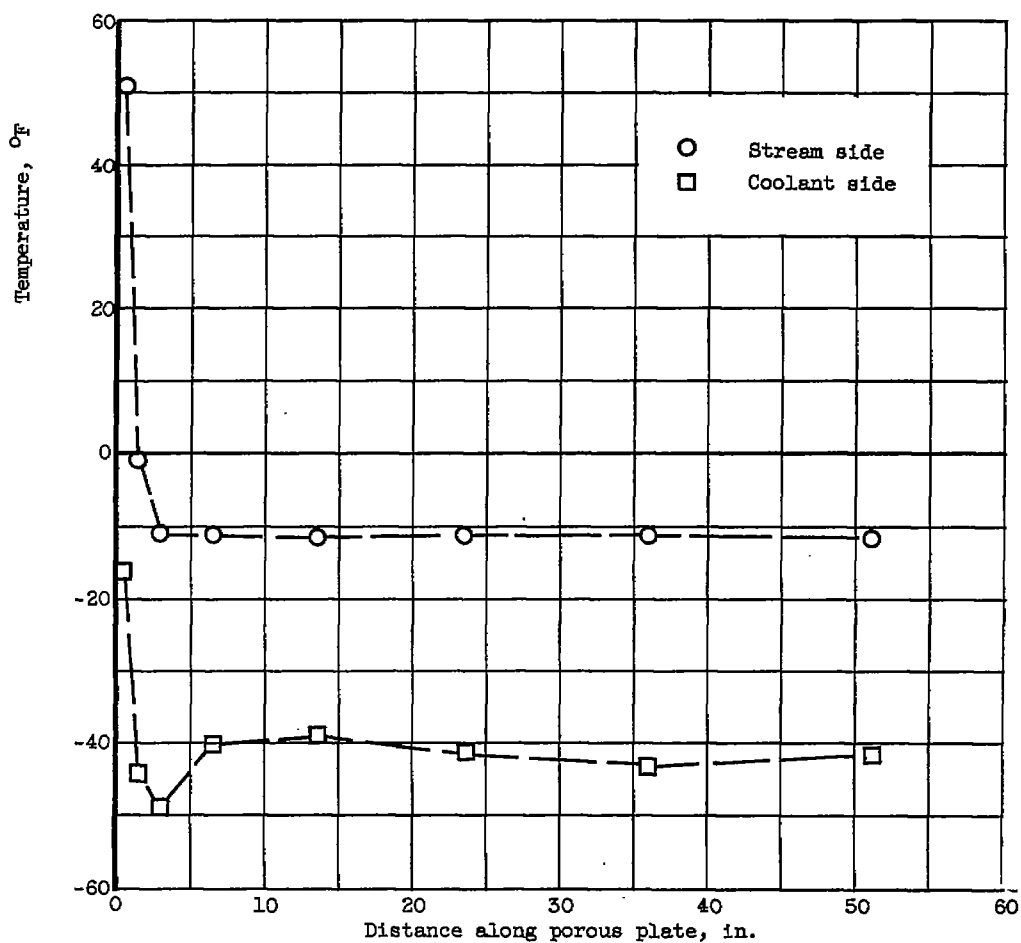
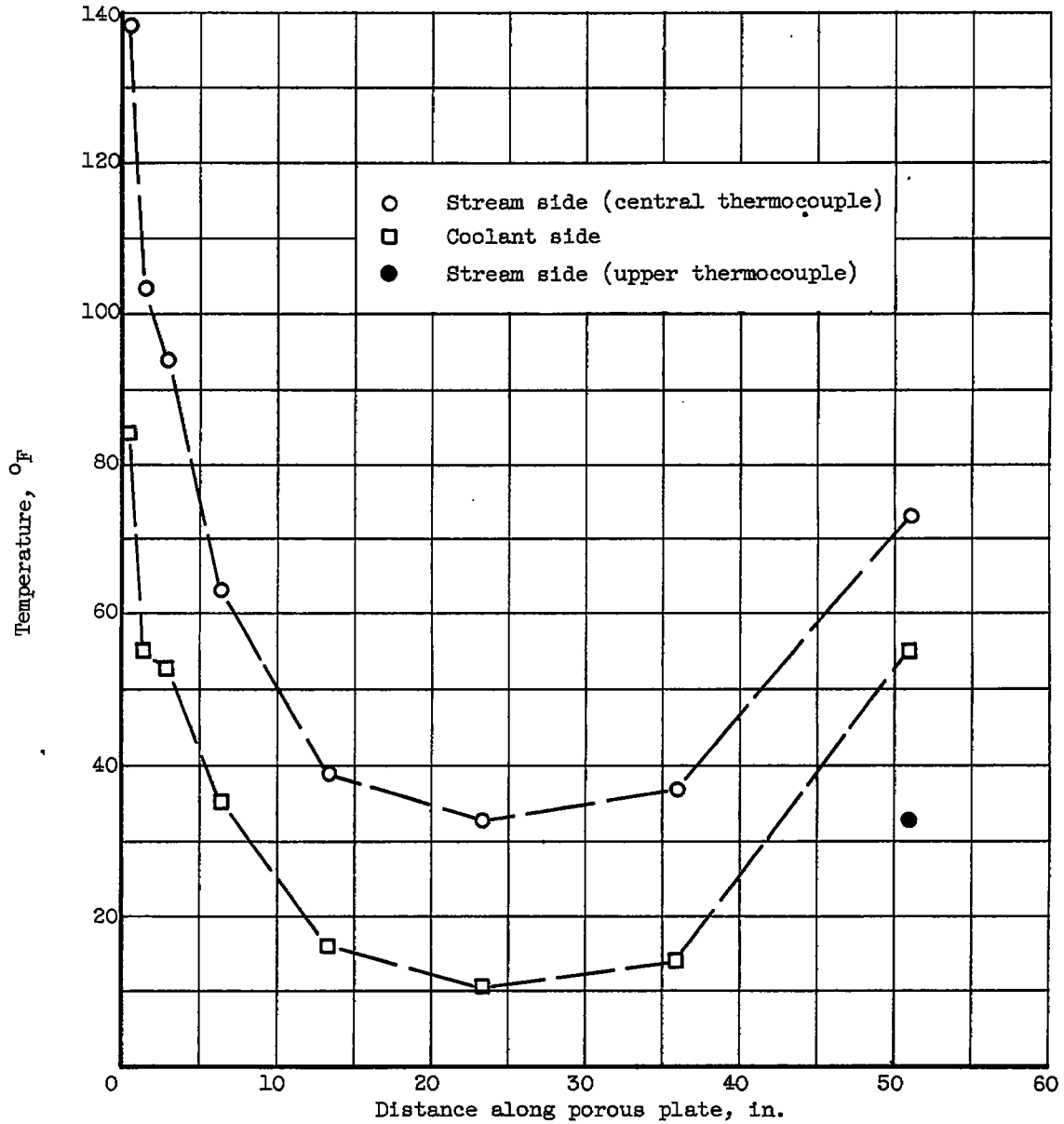□   Coolant side

(b) Maximum boundary-layer bleed. Stagnation temperature, 215° F.

Figure 7. - Temperature distributions along both stream and coolant sides of porous plate for typical constant-wall-temperature runs. Coolant temperature, -64° F.

4291
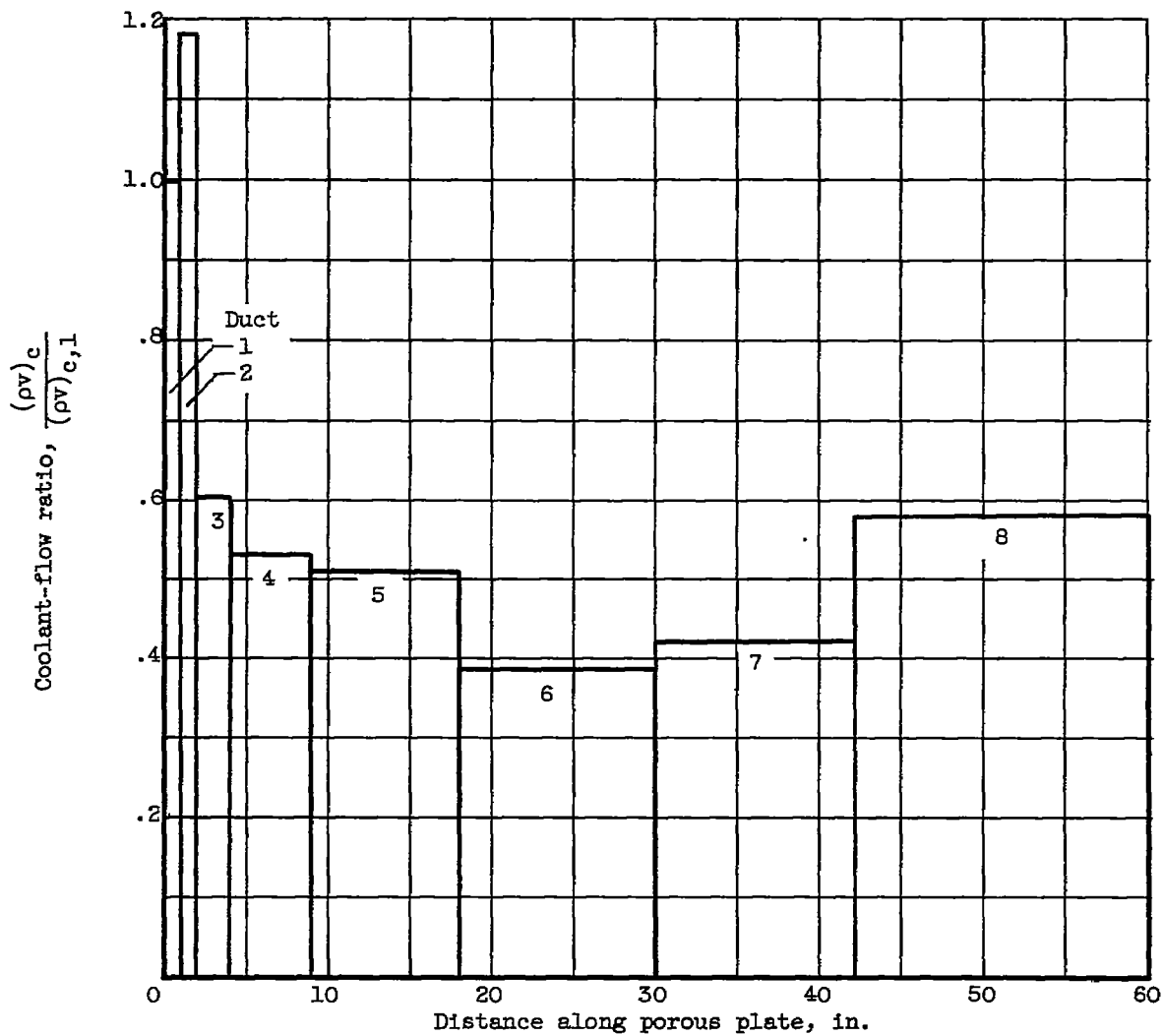
(a) No boundary-layer bleed.

Figure 8. - Coolant mass flow per unit area through ducts relative to flow through duct 1 for typical constant-wall-temperature runs.
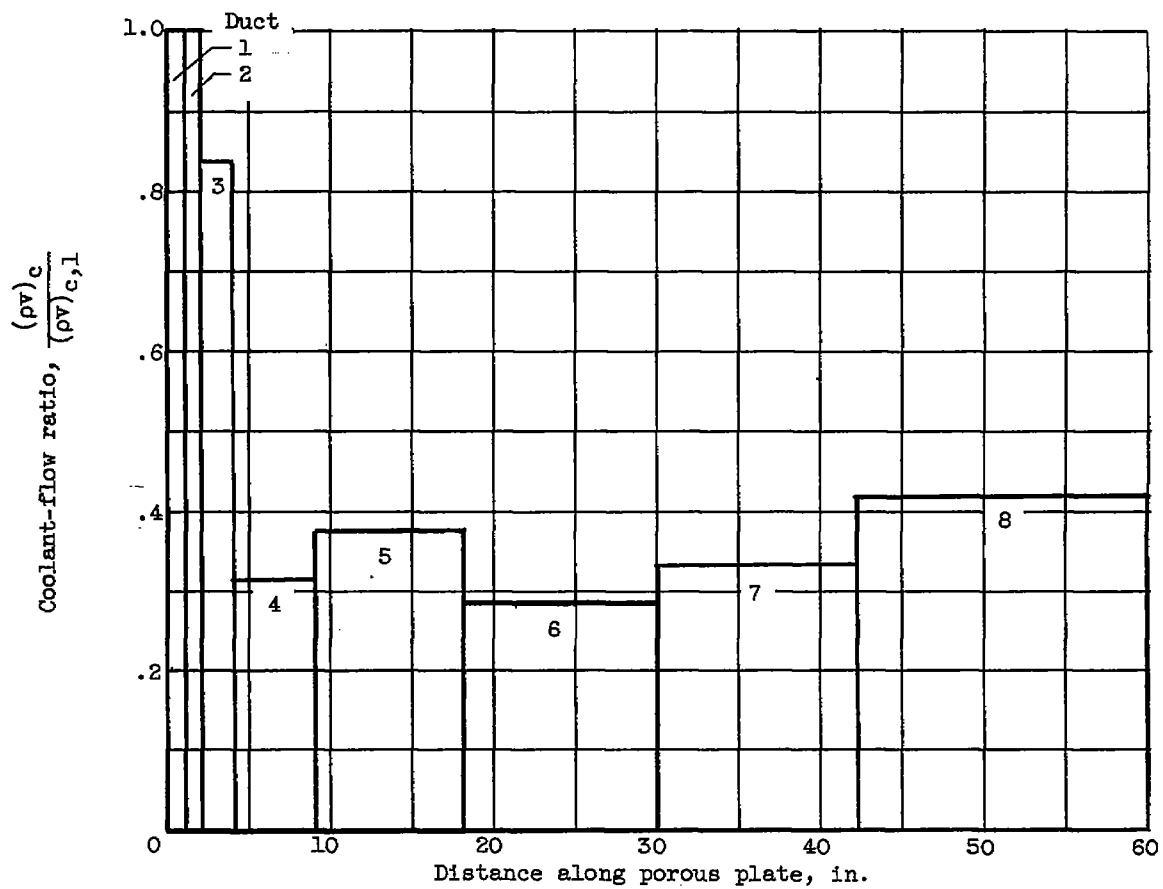
(b) Maximum boundary-layer bleed.

Figure 8. - Concluded. Coolant mass flow per unit area through ducts rela-
tive to flow through duct 1 for typical constant-wall-temperature runs.
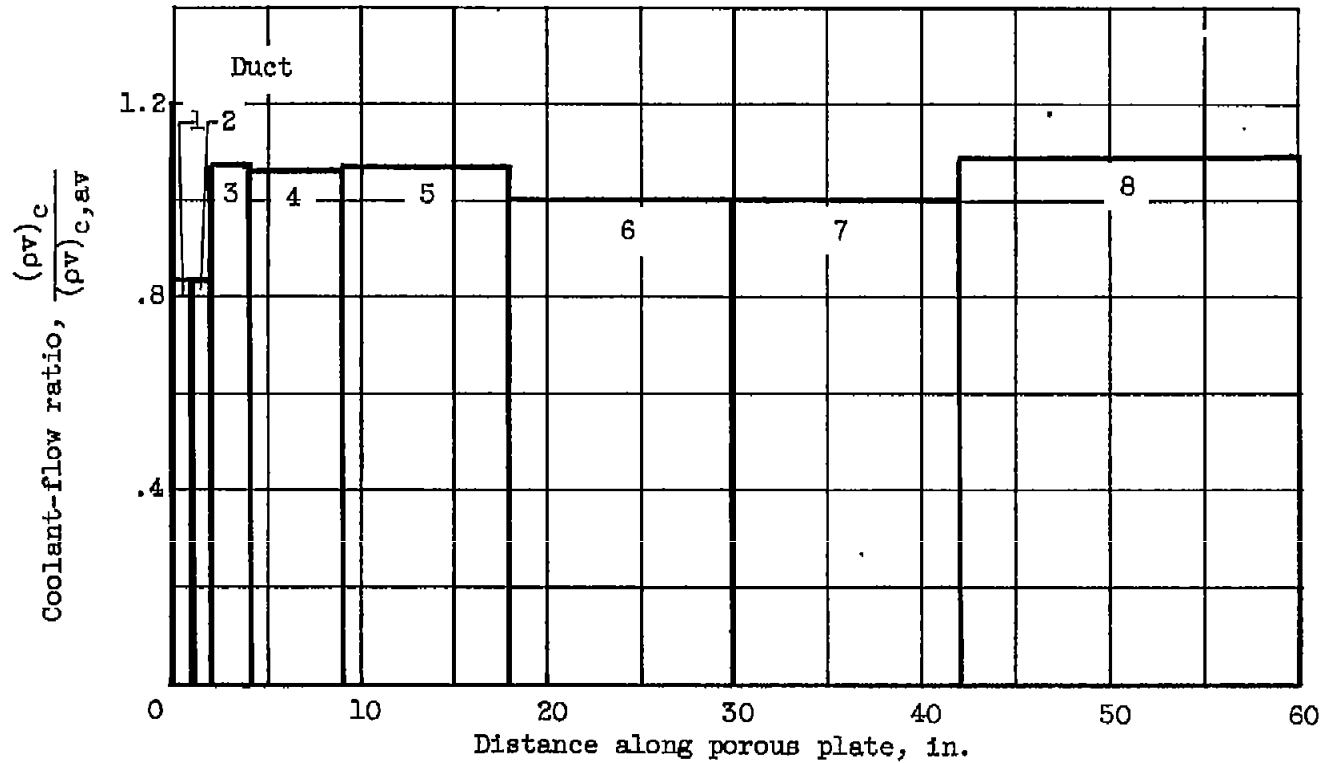
Figure 9. - Coolant mass flow per unit area through duct relative to average mass flow through all ducts for typical constant-mass-flow run.

Figure 10. - Temperature distribution along both stream and coolant sides
of the porous plate for typical constant-mass-flow run. Stagnation tem-
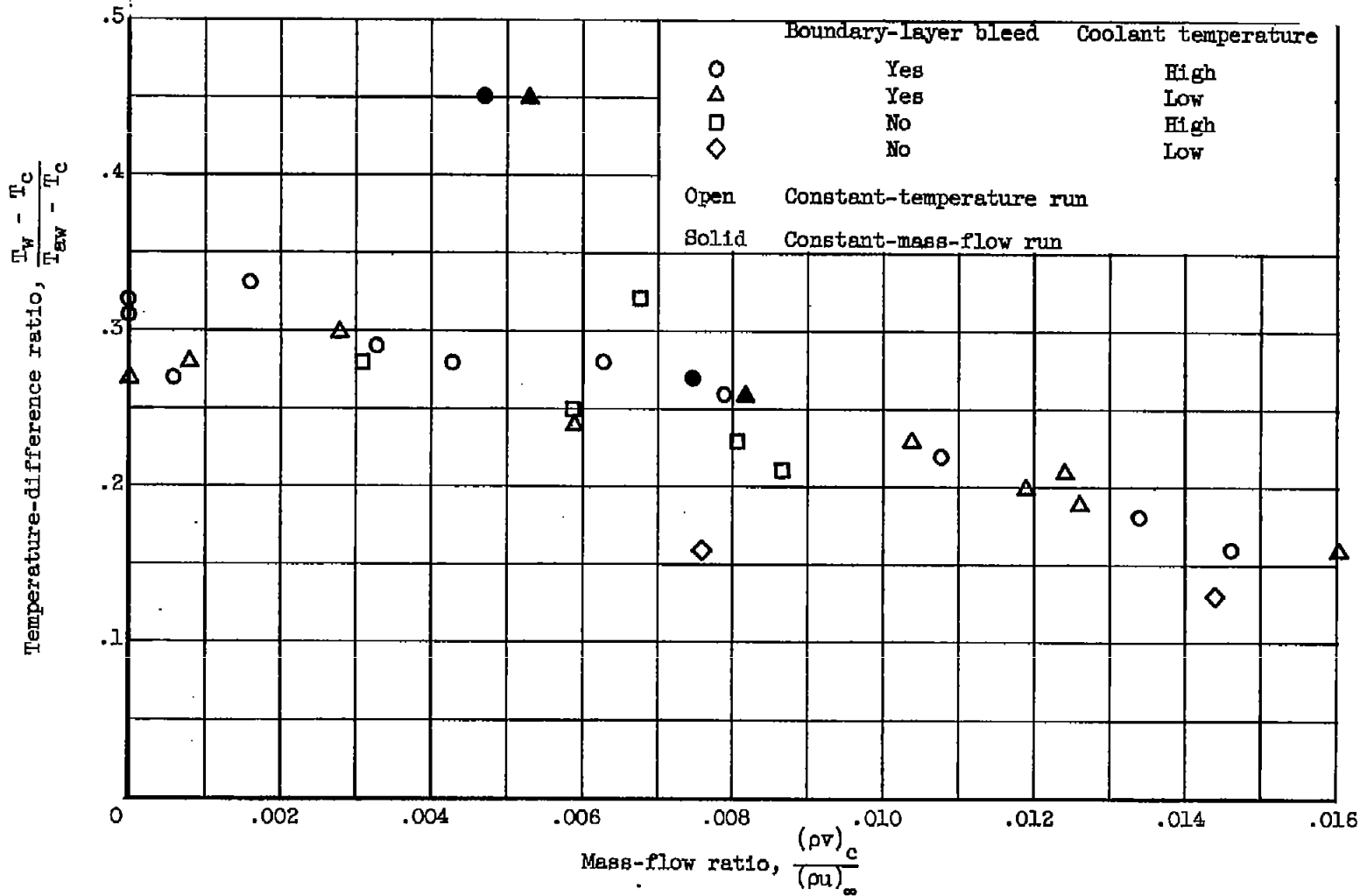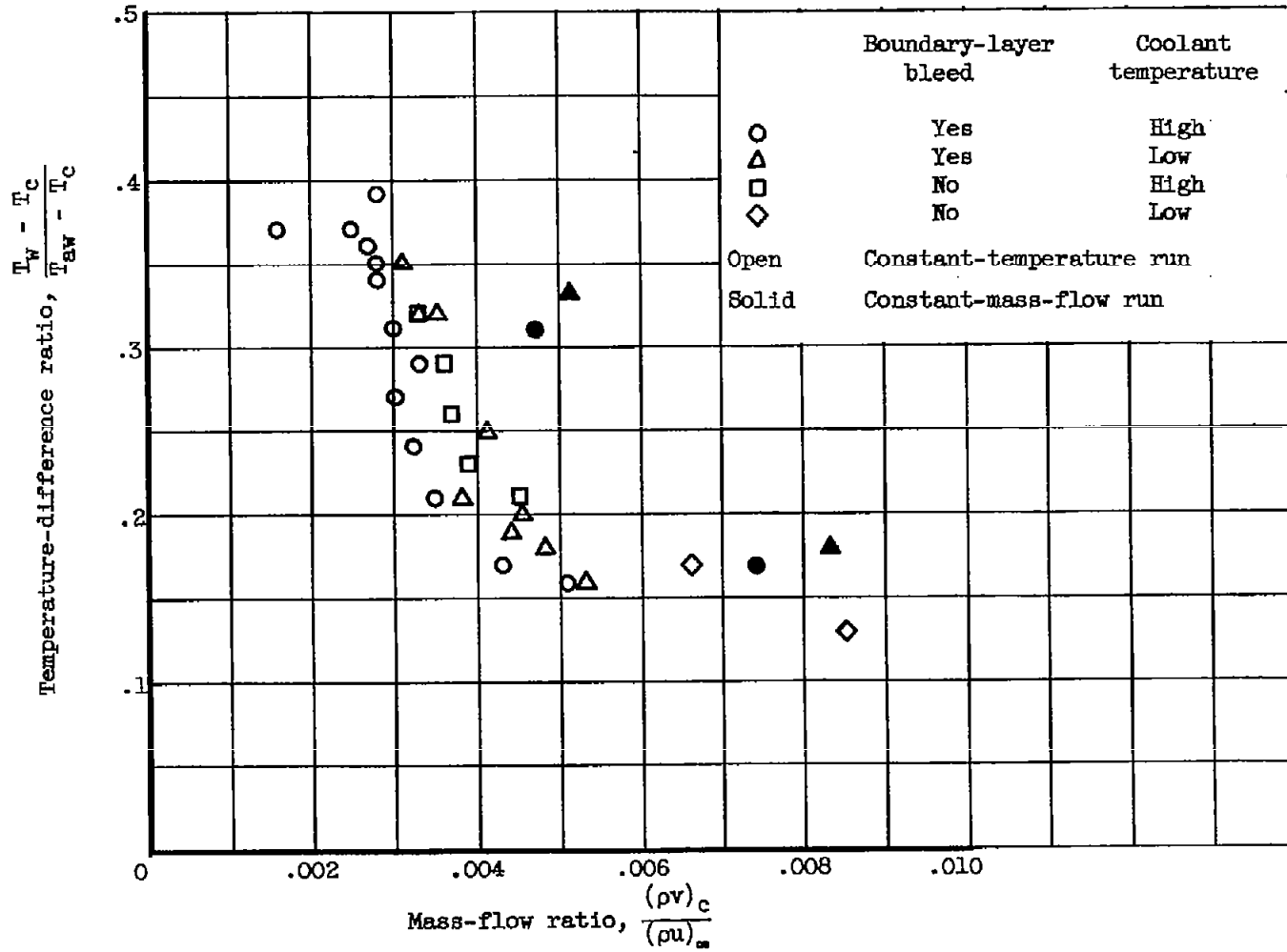perature, 215° F; coolant temperature, -15° F.
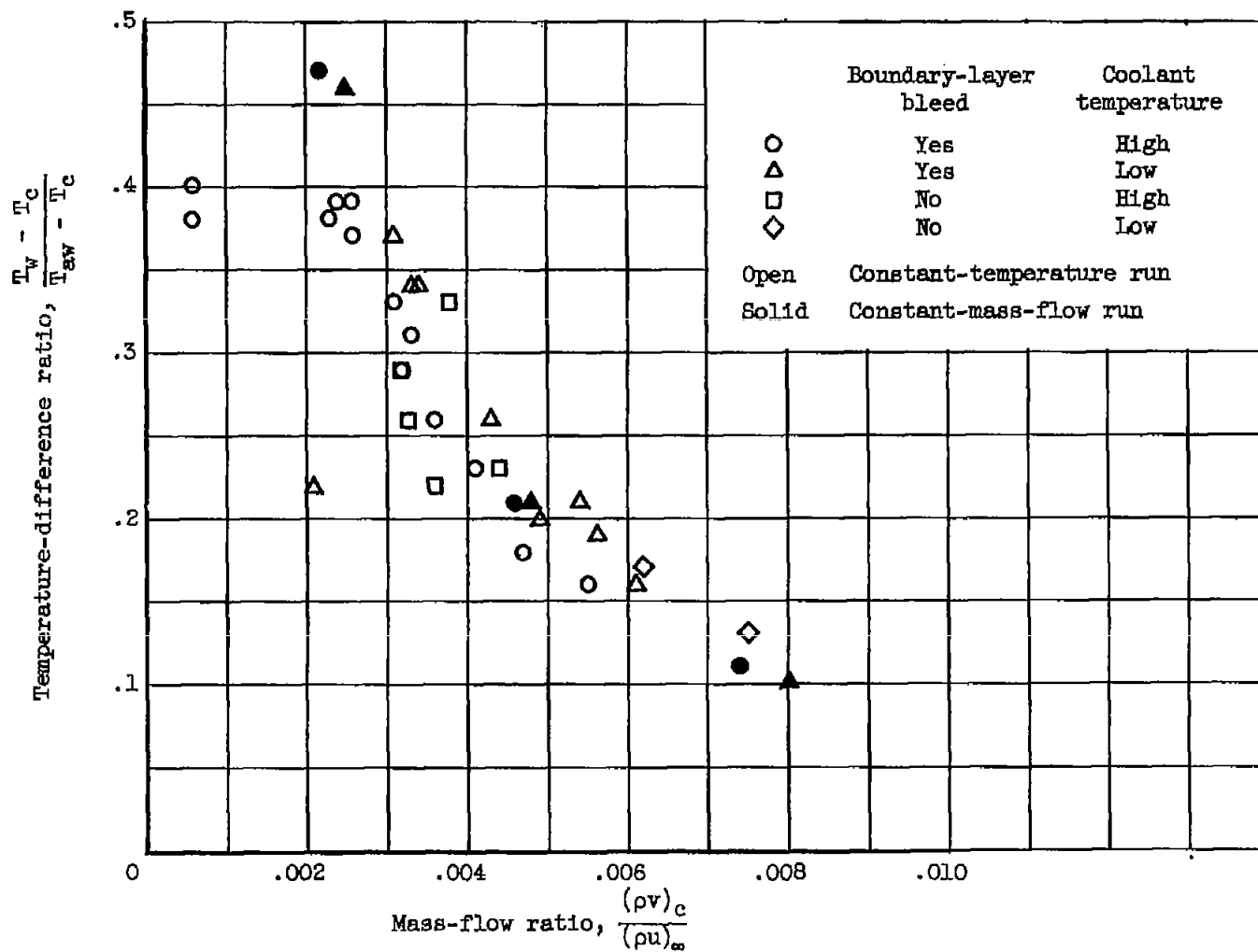
(a) Duct 3.

Figure 11. - Variation of temperature-difference ratio with mass-flow ratio based on local conditions using the central thermocouple readings.

(b) Duct 4.

Figure 11. - Continued. Variation of temperature-difference ratio with mass-flow ratio based on local conditions using the central thermocouple readings.
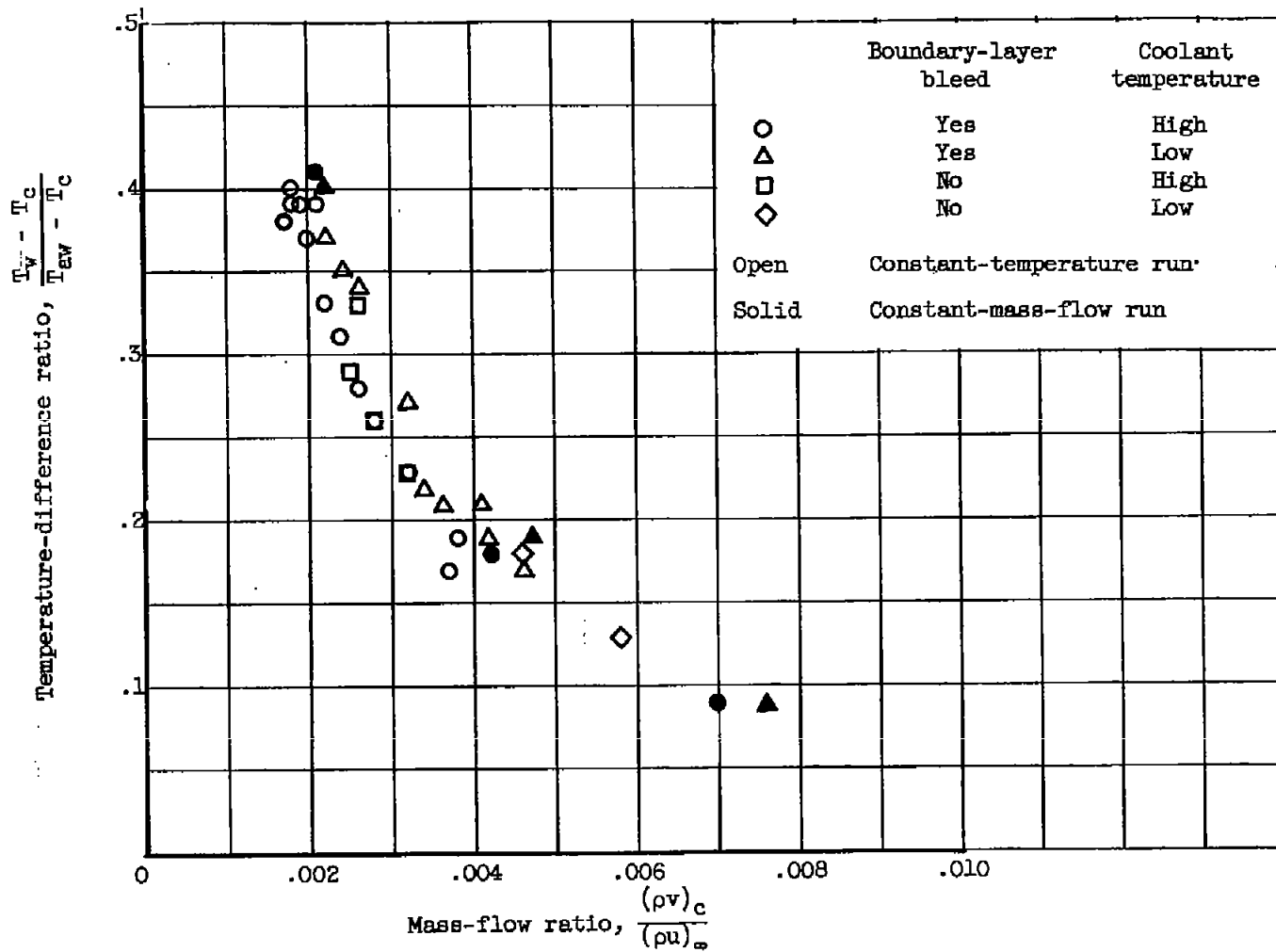
(c) Duct 5.

Figure 11. - Continued. Variation of temperature-difference ratio with mass-flow ratio based on local conditions using the central thermocouple readings.

Boundary-layer bleed	Coolant temperature
○ Yes	High
△ Yes	Low
□ No	High
◇ No	Low
Open	Constant-temperature run·
Solid	Constant-mass-flow run

$$\text{Temperature-difference ratio, } \frac{T_w - T_c}{T_{ew} - T_c}$$

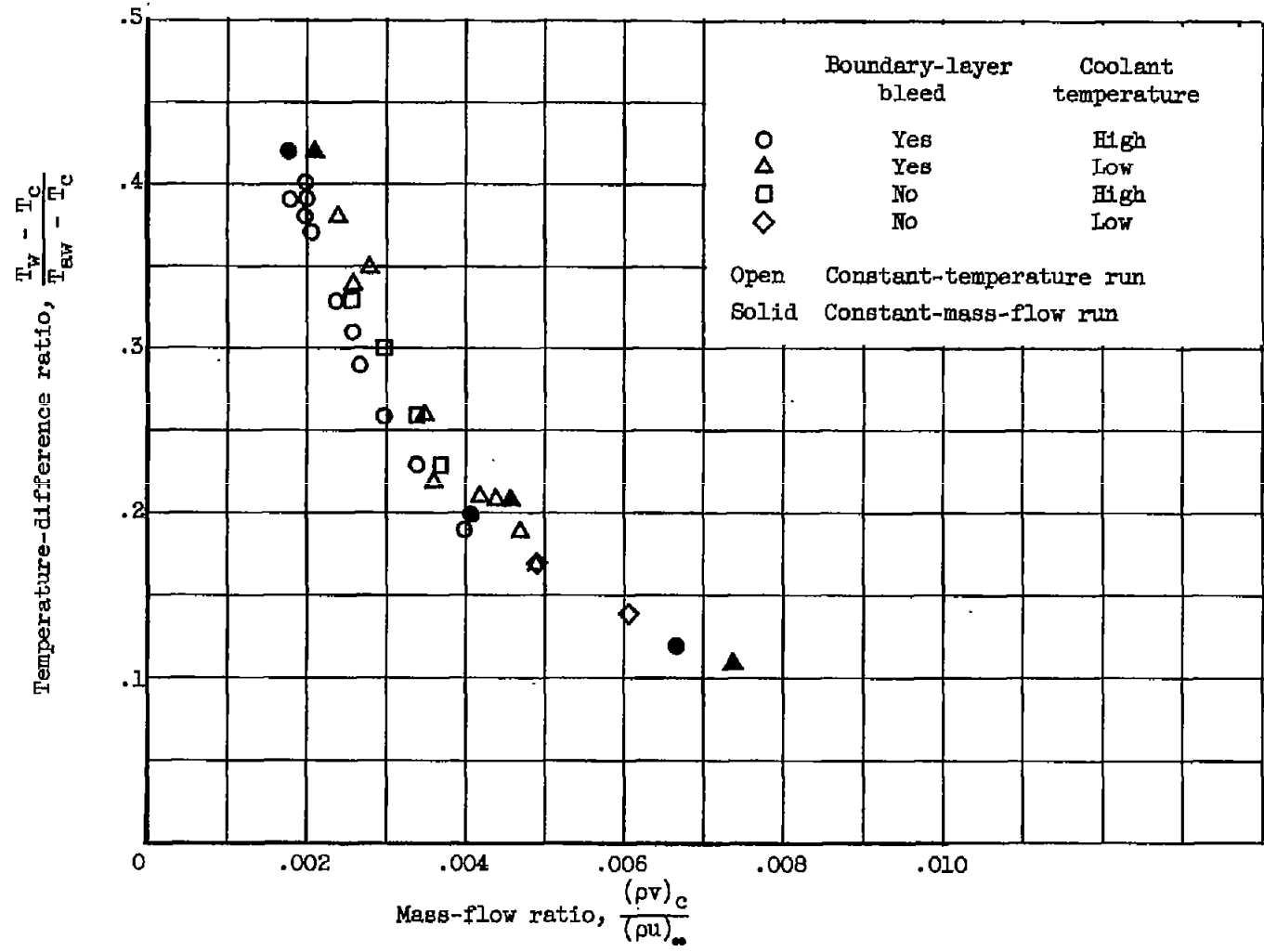$$\text{Mass-flow ratio, } \frac{(\rho v)_c}{(\rho u)_\infty}$$

(d) Duct 6.

Figure 11. - Continued. Variation of temperature-difference ratio with mass-flow
ratio based on local conditions using the central thermocouple readings.

(e) Duct 7.

Figure 11. - Continued. Variation of temperature-difference ratio with mass-flow ratio based on local conditions using the central thermocouple readings.
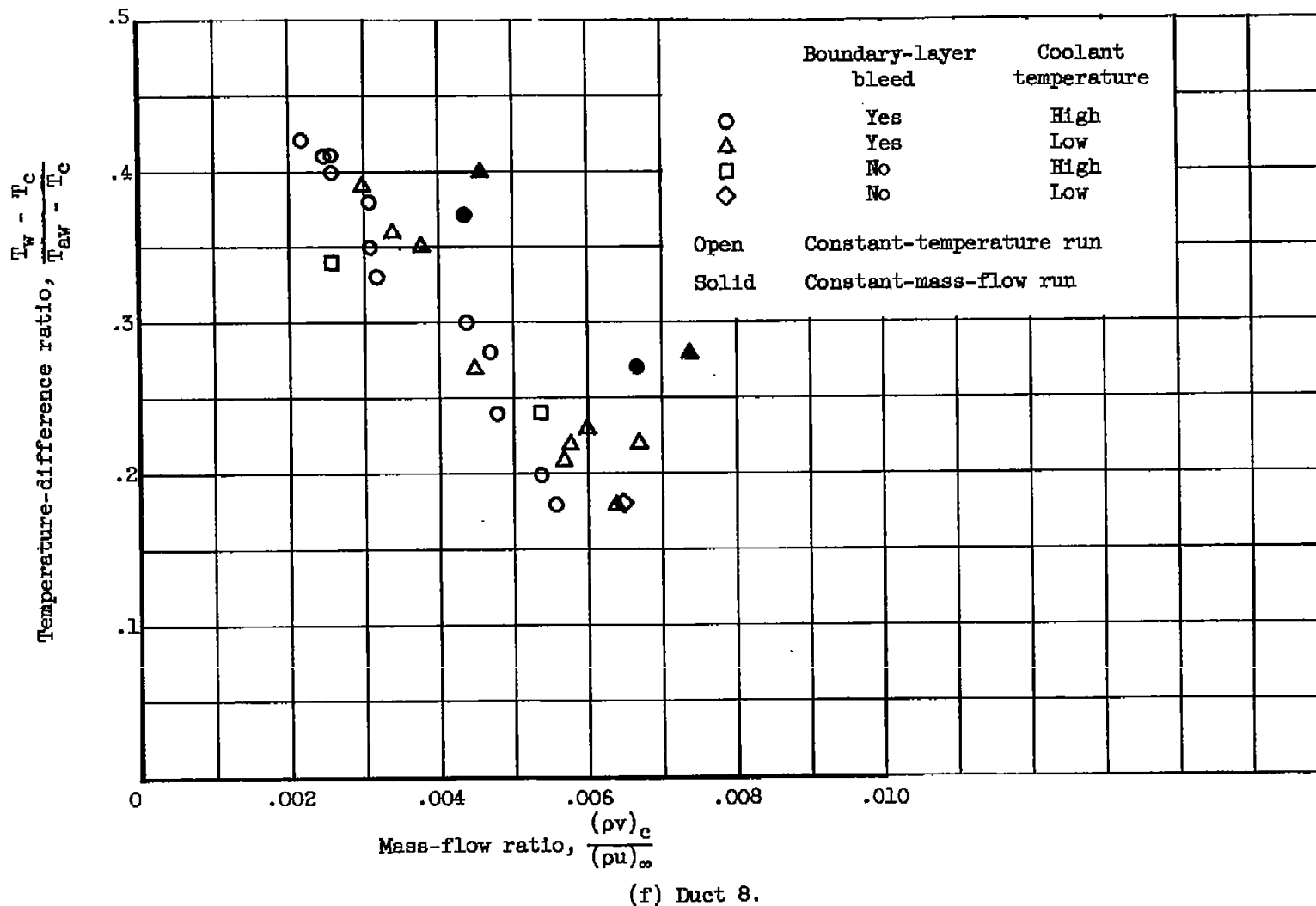
Temperature-difference ratio, $\dfrac{T_w - T_c}{T_{aw} - T_c}$

Mass-flow ratio, $\dfrac{(\rho v)_c}{(\rho u)_\infty}$

	Boundary-layer bleed	Coolant temperature
O	Yes	High
△	Yes	Low
□	No	High
◇	No	Low

Open — Constant-temperature run

Solid — Constant-mass-flow run

(f) Duct 8.

Figure 11. - Concluded.   Variation of temperature-difference ratio with mass-flow ratio based on local conditions using the central thermocouple readings.
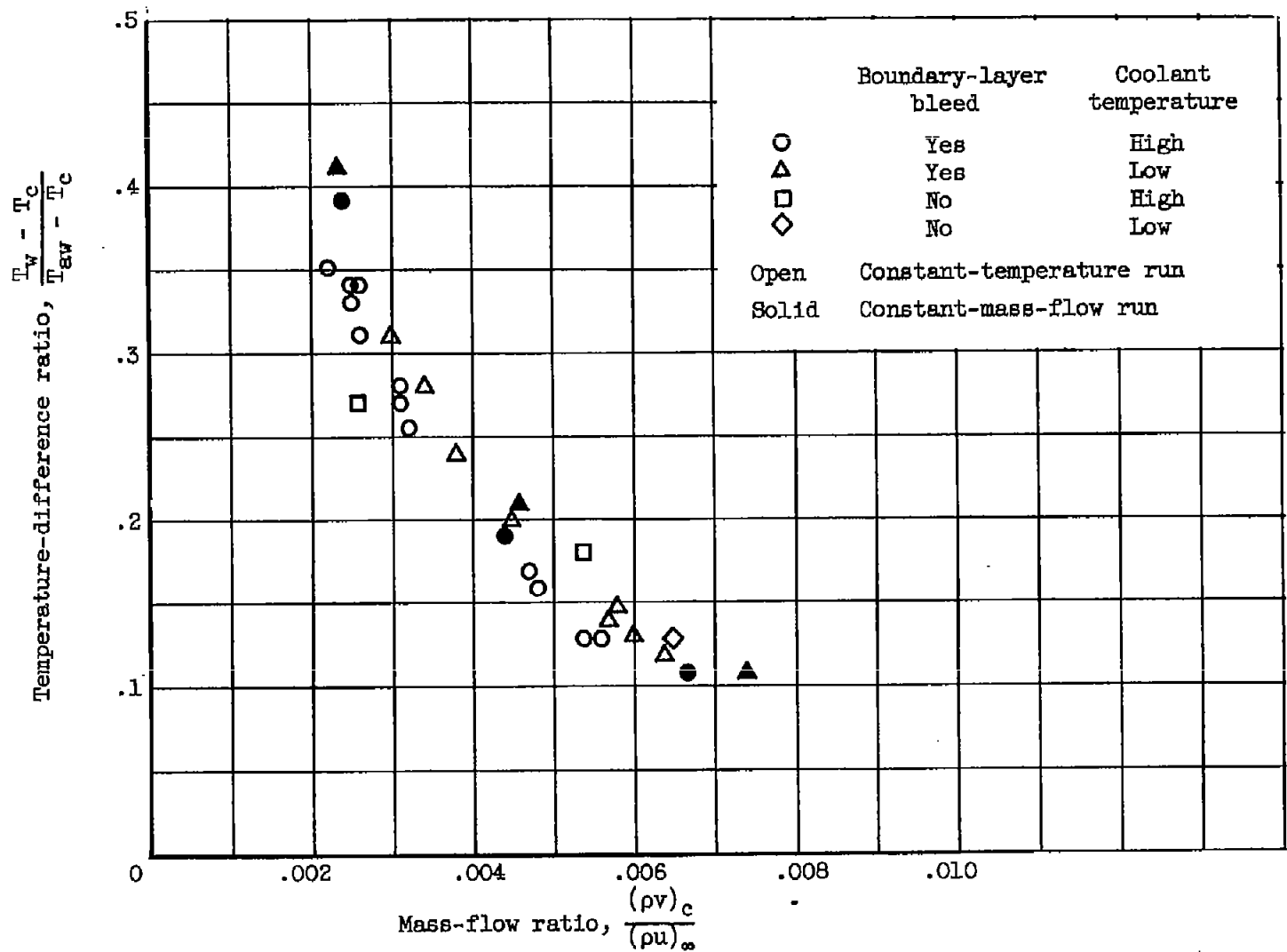
.5

Temperature-difference ratio, $\dfrac{T_w - T_c}{T_{aw} - T_c}$

	Boundary-layer bleed	Coolant temperature
O	Yes	High
△	Yes	Low
□	No	High
◇	No	Low

Open   Constant-temperature run

Solid   Constant-mass-flow run

.4

.3

.2

.1

0   .002   .004   .006   .008   .010

Mass-flow ratio, $\dfrac{(\rho v)_c}{(\rho u)_\infty}$

Figure 12. - Variation of temperature-difference ratio with mass-flow ratio for duct 8 based on local conditions using the upper thermocouple reading.
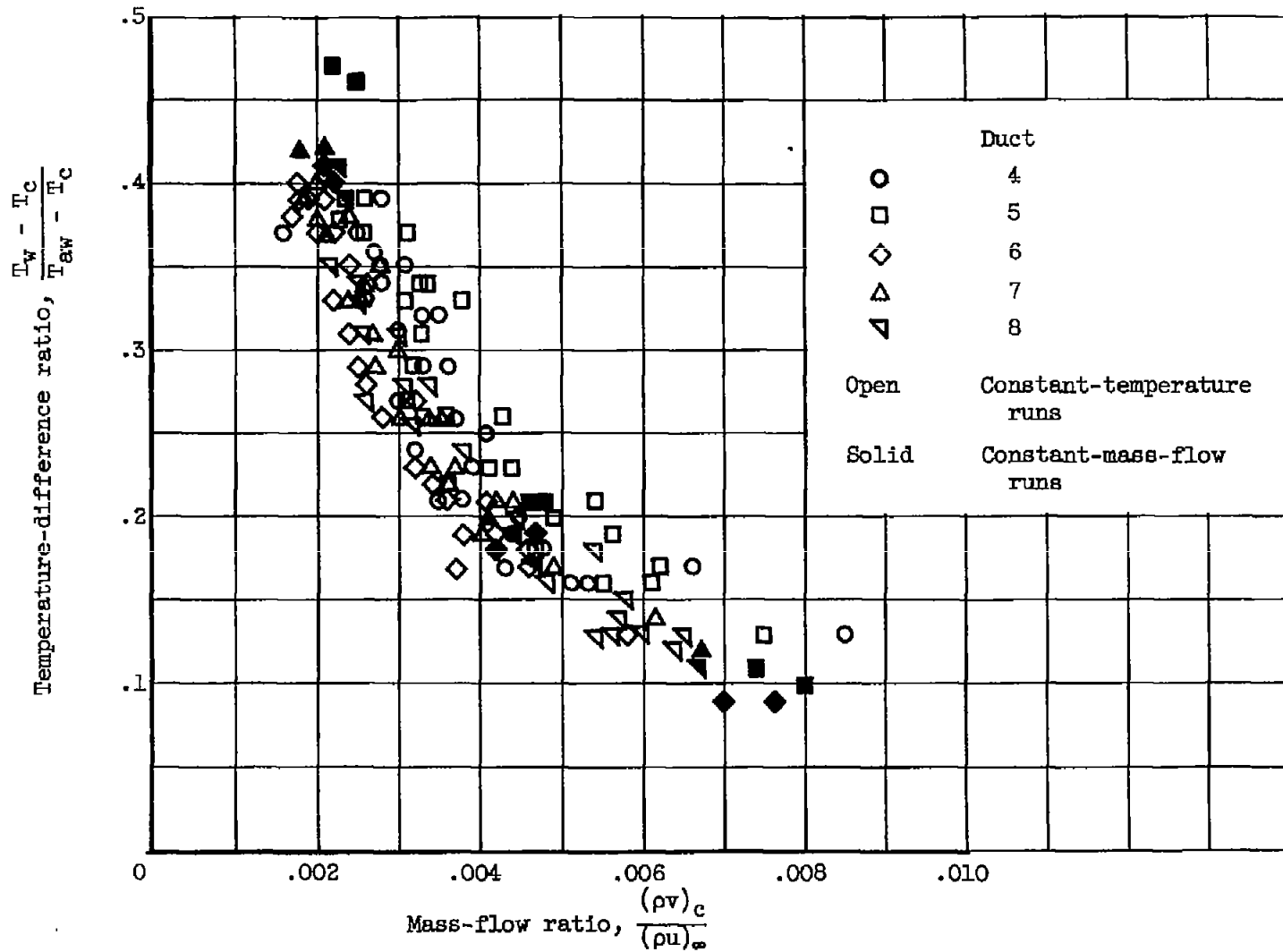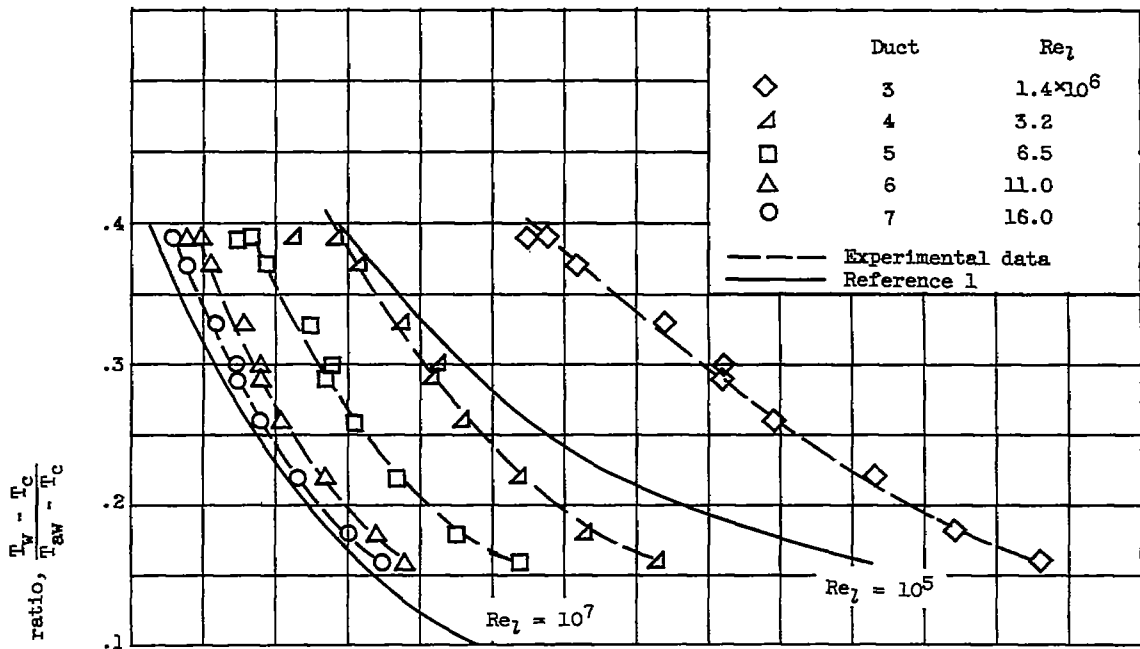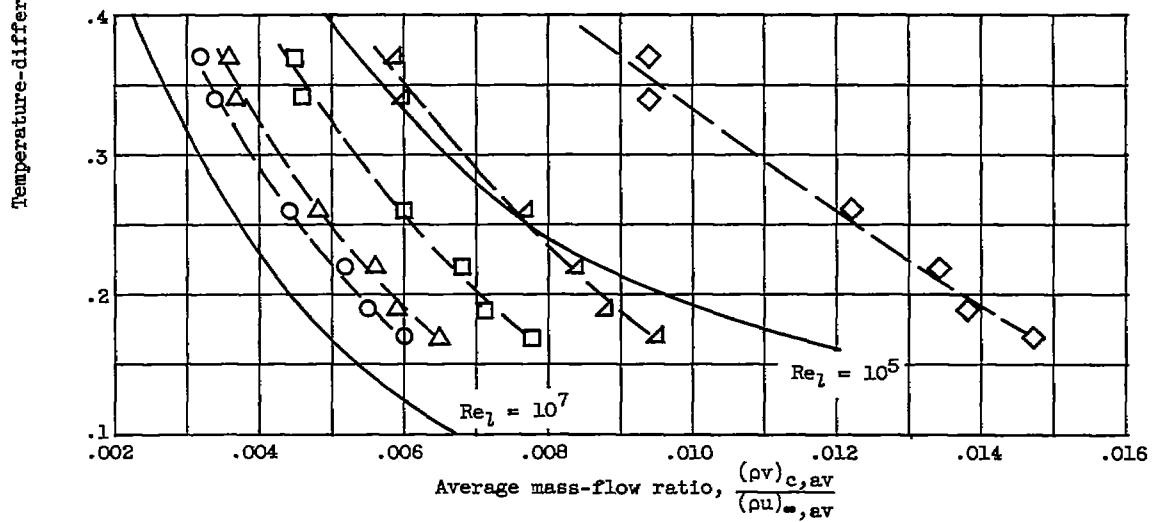
Figure 13. - Variation of temperature-difference ratio with mass-flow ratio based on local conditions for ducts 4 to 8.

Figure 14. – Comparison of theoretical and experimental results based on average conditions along porous plate for runs with maximum boundary-layer bleed.